To appear in the *International Journal of Control*
Vol. 00, No. 00, Month 20XX, 1–24

Multistage Output-lifting Eigenstructure Assignment: A Multirate Ball and Plate Example

L. Chen[a*] , A.J. Pomfret[b] and T. Clarke[b]

[a] *College of Engineering, Mathematics and Physical Sciences, University of Exeter, UK;* [b] *Department of Electronic Engineering, University of York, UK*

(*Received 00 Month 20XX; accepted 00 Month 20XX*)

By exploiting both the left and the right allowable subspaces in consecutive stages, this paper extends a recently-developed output-lifting eigenstructure assignment approach into a multistage eigenstructure assignment scheme. In this scheme, design degrees of freedom, enlarged via output-lifting, are further exploited to improve eigenvector assignment. To mitigate the inherent conflicts between the theoretical development of eigenstructure assignment and inherent physical system characteristics, the paper also clearly demonstrates how to derive an ideal eigenstructure, particularly the desired eigenvectors, to distribute and decouple the natural modes among appropriate states or outputs, based upon an example: a novel multirate Ball and Plate system. The design and simulation results show the efficacy of the scheme.

Keywords: lifting; eigenstructure assignment; ball and plate system; allowable subspace

*Corresponding author. Email: Lejun.Chen@exeter.ac.uk

Nomenclature

The reader is referred to Figures 1 to 3.

a	Length of the plate
b	Width of the plate
$\tilde{b}$	Damping constant of the rotational mechanical system
d	Ball displacement relative to the plate
f_x	External force applied at x
f_y	External force applied on y
h	Ball vertical displacement along $\vec{ok}$
I_i	Armature current flow into the ith motor
J_b	Moment of Inertial of the ball
J_m	Moment of inertia of the rotor
J_p	Moment of Inertial of the plate
K_e	Motor constant related to the back electromotive force
K_t	Electromotive force constant
l	Length of the motor shaft
L_a	Armature induction
m	Mass of the ball
m_{ω_x}	Moment applied to the ball along ω_x
m_{ω_y}	Moment applied to the ball along ω_y
$\tilde{p}$	Plate angular velocity along $\vec{oi}$
$\tilde{q}$	Plate angular velocity along $\vec{oj}$
$\tilde{r}$	Plate angular velocity along $\vec{ok}$
r_b	Radius of the ball
R_m	Armature resistance
s	Ball displacement relative to the earth
$\bar{s}_1$	Ball displacement along $\vec{oi}$
$\bar{s}_2$	Ball displacement along $\vec{oj}$
V_i	Input voltage applied to the armature of the ith motor
x	Ball displacement along $\vec{ol}$
y	Ball displacement along $o\vec{m}n$
Z_i	Vertical displacements of three push-rods
α_i	Rotation angle of three DC motor
ϕ	Plate rotation angle along $\vec{ol}$
θ	Plate rotation angle along $o\vec{m}n$
ω	Ball angular velocity relative to the earth
ω_p	Plate angular velocity relative to the earth
ω_x	Ball angular velocity along $\vec{ol}$
ω_y	Ball angular velocity along $o\vec{m}n$
ω_z	Ball angular velocity along $\vec{on}$

1. Introduction

Through synthesizing a feedback gain matrix that matches the closed-loop eigenstructure as closely as possible to an ideal set, eigenstructure assignment (EA) ensures some useful properties such as stability robustness, desired transient response, mode decoupling and disturbance rejection (Alireza & Batool, 2012; B. Chen & Nagarajaiah, 2007; Duval, Clerc, & LeGorrec, 2006; Farineau, 1989; Kshatriya, Annakkage, Hughes, & Gole, 2007; Lhachemi, Saussie, & Zhu, 2017; G. P. Liu & Pat-

ton, 1998; Y. Liu, Tan, Wang, & Wang, 2013; Moore, 1976; Ntogramatzidis, Nguyen, & Schmid, 2015; Ouyang, Richiedei, Trevisani, & Zanardo, 2012; Patton, Liu, & Patel, 1995; Piou & Sobel, 1994, 1995; Pomfret & Clarke, 2009; Wahrburg & Adamy, 2013; White, 1995; White, Bruyere, & Tsourdos, 2007). Compared with many competitive approaches that only achieve placement of the desired eigenvalues of the closed-loop system, EA additionally manipulates the direction of the eigenvectors. These define how system inputs will affect system modes and how system modes will be assigned to system states/outputs. Thus realistic control effect or the quality of control performance, e.g. the handling qualities of a flight controlled aircraft, can be achieved in a straightforward manner. Furthermore, EA ensures a 'visible' design process which may reduce time consumed in post-processing for tuning purposes. The development of EA has not been widely persued in the recent years due to a) traditional EA, particularly output feedback EA, requiring significant design degrees of freedom (DoF) (Andry, Shapiro, & Chung, 1983; Clarke, Ensor, & Griffin, 2003; Clarke & Griffin, 2004; Clarke, Griffin, & Ensor, 2003; Pomfret, Clarke, & Ensor, 2005; Roppenecker & O'Reilly, 1989; Srinathkumar, 1978; Zhao & Lam, 2016a, 2016b). b) Very few works (Clarke, Ensor, & Griffin, 2003; Garrard, Low, & Prouty, 1989; Low & Garrard, 1993) attempting to analyze how to derive an ideal eigenstructure, particularly the ideal eigenvectors, that reflect the inherent physical characteristics of the target system. This paper aims to cope with above two bottlenecks.

In the literature, Piou and Sobel (1994, 1995) developed the multirate EA approach, but the concept of 'lifting' (T. Chen & Francis, 1995) was not taken into account. The lifting framework and EA were first time combined by Patton et al. (1995) to enlarge DoF, however this approach only lifted system inputs and generated inter-sample ripple. Recently, L. Chen, Pomfret, and Clarke (2017) developed output lifting EA which largely improved DoF and the single-rate full state feedback eigenstructure can be assigned in an output feedback framework, particularly when the Kimura condition (Kimura, 1975) is not satisfied.

In this paper, a multi-stage output-lifting EA scheme is developed. It is well known that for a single-stage EA, there always exist the inherent conflicting nature of the right and left EA. Once the right EA of the system is determined, the left EA is determined of itself, and vice versa. One of the benefits of using the multistage EA is that both the properties of left and right EA can be exploited. For example, mode decoupling and disturbance decoupling can be achieved using the right EA, whilst the control efforts, controllability measure and the disturbance suppression can be taken into account using the left EA. In more details, if the left modal matrix are chosen to be parallel to the columns of the system input matrix, or at least, in the least square sense, the control efforts will be small. Also if the left modal matrix are selected to be orthogonal to the disturbance distribution matrix, disturbance could be well suppressed. Additionally, unlike the right EA, directly assigning the left eigenstructure in a single-stage as right EA could fail even in a full state feedback case, and the achieved closed-loop eigenvalues may not coincide with the desired eigenvalues. This is due to the fact that system B-matrix is not square in general and the gain matrix is obtained only in the least square sense.

In the scheme of the multistage EA, the eigenvalues assigned using the right EA in the first stage will be protected before the start of the second stage. This eigenvalue protection progress leads to a reduced order system where the number of effective system outputs are reduced by the number of eigenvalues assigned in the first stage and the elements associated with each left eigenvector cannot be exactly assigned even if the system is full state feedback. Exploiting the fact that output-lifting has the capability to enlarge the number of effective system outputs, the dimension of the left allowable subspace is thus increased and a left allowable subspace based eigenvector assignment can improve achieved eigenvectors and allows more elements of each eigenvector to be exactly assigned in the second stage. More details will be discussed in the sequel.

To mitigate the inherent conflict between the *theoretical* development of EA with the *actual* system inherent physical characteristics, this paper also clearly demonstrates how to derive an ideal eigenstructure based upon a genuine example of a novel mutirate Ball and Plate system. Not only are the natural modes of Ball and Plate system decoupled and distributed in appropriate states

or outputs, but also the eigenvectors are derived to be consistent with the physical relationships between Ball and Plate system states. Due to an otherwise lack of DoF, multistage output-lifting EA is applied to Ball and Plate system.

The main contributions of the paper are a) enhancing the DoF induced by output-lifting using multistage EA. Eigenvector assignment can be improved through the exploitation of the enlarged left allowable subspace. b) demonstration of how to determine a practical eigenstructure using a Ball and Plate system example. Compared with other methods described in the literature (Garrard et al. (1989); Low and Garrard (1993)), a more transparent approach to selecting a set of ideal eigenvectors, parameterised by the desired eigenvalues, is developed in this paper.

The remainder of the paper is outlined as follows: Section 2 briefly introduces output-lifting EA, followed by the development of multistage output-lifting EA in Section 3. The mathematical model of a Ball and Plate system is developed in Section 4. Section 5 describes how the derive an ideal eigenstructure based upon the system physical characteristics. In Section 6, multistage output-lifting EA is then applied to this Ball and Plate system. The design and simulation results demonstrate the efficacy of the scheme.

2. Output-lifting eigenstructure assignment

In this section, the output-lifting EA approach (L. Chen et al., 2017) will be introduced briefly. Consider a discrete-time, controllable and observable linear time-invariant system

$$\begin{aligned} \dot{x} &= Ax + Bu \\ y &= Cx + Du \end{aligned} \tag{1}$$

where $A \in \mathbb{R}^{n\times n}, B \in \mathbb{R}^{n\times r}, C \in \mathbb{R}^{m\times n}$ and $D \in \mathbb{R}^{m\times r}$ are matrices with $\text{rank}(B) = r$ and $\text{rank}(C) = m$. Suppose the system in (1) is discretized at the base sampling period T_b which is any common factor of the input and output sampling periods. Furthermore, the hold circuit and the sampler work with sample periods of $q_i T_b$ and $p_o T_b$ respectively. Then the main sampling period of the system becomes $T = \text{l.c.m}(p_o, q_i) * T_b$ where l.c.m stands for least common multiple. Suppose system inputs and outputs are lifted by q and p respectively, where

$$q = \frac{l.c.m(p_o, q_i)}{q_i} \quad \text{and} \quad p = \frac{l.c.m(p_o, q_i)}{p_i} \tag{2}$$

denote the input ratio and the output ratio, respectively. As in T. Chen and Francis (1995), a controllable and observable lifted system has the form

$$\begin{aligned} x(k+1) &= A_L x(k) + B_L \bar{u}(k) \\ \bar{y}(k) &= C_L x(k) + D_L \bar{u}(k) \end{aligned} \tag{3}$$

where $x(k) := x(kT)$. In (3), lifted inputs $\bar{u}(k)$ and outputs $\bar{y}(k)$ are

$$\bar{u}(k) := \begin{bmatrix} u(kT) \\ u(kT + pT_b) \\ u(kT + 2pT_b) \\ \vdots \\ u(kT + (pq - p)T_b) \end{bmatrix} \quad \bar{y}(k) := \begin{bmatrix} y(kT) \\ y(kT + qT_b) \\ y(kT + 2qT_b) \\ \vdots \\ y(kT + (pq - q)T_b) \end{bmatrix} \tag{4}$$

and the matrices $A_L \in \mathbb{R}^{n\times n}, B_L \in \mathbb{R}^{n\times qr}, C_L \in \mathbb{R}^{pm\times n}$ and $D_L \in \mathbb{R}^{pm\times qr}$ are

$$\left[\begin{array}{c|c} A_L & B_L \\ \hline C_L & D_L \end{array}\right] := \left[\begin{array}{c|cccc} A^{pq} & \sum_{i=pq-p}^{pq-1} A^i B & \sum_{i=pq-2p}^{pq-p-1} A^i B & \cdots & \sum_{i=0}^{p-1} A^i B \\ \hline C & D_{0,0} & D_{0,1} & \cdots & D_{0,q-1} \\ CA^q & D_{1,0} & D_{1,1} & \cdots & D_{1,q-1} \\ CA^{2q} & D_{2,0} & D_{2,1} & \cdots & D_{2,q-1} \\ \vdots & \vdots & \vdots & \ddots & \vdots \\ CA^{pq-q} & D_{p-1,0} & D_{p-1,1} & \cdots & D_{p-1,q-1} \end{array}\right] \tag{5}$$

where the element $D_{i,j}$ is defined as

$$D_{i,j} = D\mathcal{X}_{[jp,(j+1)p)}(iq) + \sum_{h=jp}^{(j+1)p-1} CA^{in-1-h}B\mathcal{X}_{[0,iq)}(h) \tag{6}$$

and the characteristic function on integers $\mathcal{X}_{[a,b)}(h)$ is

$$\mathcal{X}_{[a,b)}(h) = \begin{cases} I & a \le h < b \\ 0 & \text{otherwise} \end{cases}$$

From (5), the number of effective system inputs and outputs are enlarged (i.e. $r \to qr$ and $m \to pm$) and therefore extra DoF may be parameterised for the synthesis of the gain matrix $K \in \mathbb{R}^{r\times pm}$. In this paper, the eigenvalues are assumed to be self-conjugate and pole-assignable. This assumption ensures the gain matrix K is real (Kimura, 1977). Applying an static output feedback law $\bar{u}(k) = K\bar{y}(k) + \bar{r}(k)$ to (3) yields the closed-loop system

$$\begin{aligned} x(k+1) &= (A_L + B_L N C_L)x(k) + (B_L + B_L N D_L)\bar{r}(k) \\ \bar{y}(k) &= (C_L + D_L N C_L)x(k) + (D_L + D_L N D_L)\bar{r}(k) \end{aligned} \tag{7}$$

where $\bar{r}$ represents lifted exogenous inputs and

$$N = (I - KD_L)^{-1}K \tag{8}$$

Using the fact that the ith distinct closed-loop right eigenpair (a pair of eigenvalue and eigenvector), i.e. λ_i and v_i, satisfies

$$(A_L + B_L N C_L)v_i = \lambda_i v_i \tag{9}$$

$$0 = [A_L - \lambda_i I \quad B_L] \begin{bmatrix} v_i \\ NC_L v_i \end{bmatrix} \tag{10}$$

and therefore $\begin{bmatrix} v_i \\ NC_L v_i \end{bmatrix}$ belongs to the nullspace of $[A_L - \lambda_i I \quad B_L]$ i.e. the right allowable subspace. For some $f_i \in \mathbb{C}^{qr\times 1}$,

$$\begin{bmatrix} v_i \\ NC_L v_i \end{bmatrix} = \begin{bmatrix} P_i \\ Q_i \end{bmatrix} f_i \tag{11}$$

where

$$\text{range}\left(\begin{bmatrix} P_i \\ Q_i \end{bmatrix}\right) = \text{null}([A_L - \lambda_i I \quad B_L]) \tag{12}$$

and $P_i \in \mathbb{C}^{n\times qr}$ is an orthonormal basis of the right allowable subspace used to select v_i and $Q_i \in \mathbb{C}^{qr\times qr}$. Once the design vector f_i has been established, the matrices V, S are calculated via

$$\begin{aligned} V &= [v_1 \dots v_n] = [P_1 f_1, \dots, P_n f_n] \\ S &= NC_L V = [Q_1 f_1, \dots, Q_n f_n] \end{aligned} \tag{13}$$

Suppose it follows from (5) that $pm \geq n$, then substituting (8) into (13) yields

$$S = (I - KD_L)^{-1} KC_L V = K(D_L S + C_L V) \tag{14}$$

and the gain matrix can be calculated as

$$K = S(C_L V + D_L S)^{\dagger} + \Xi(I - (C_L V + D_L S)(C_L V + D_L S)^{\dagger}) \tag{15}$$

where $(\cdot)^{\dagger}$ is the Moore-Penrose inverse operation and Ξ is the free matrix to be parameterised.

Remark 2.1: *From (10), the dimension of the right allowable subspace corresponding to an output-lifting system ($q = 1$) is r due to $rank(B_L) = r$, and therefore output-lifting does not enlarge the dimension of the allowable right subspace compared with one associated with full state feedback. The maximum number of exaclty assignable elements of each eigenvector is r.*

3. Multistage output-lifting eigenstructure assignment

This section further exploits DoF induced by output-lifting EA. Instead of using only the right allowable subspace, the left allowable subspace with an increased dimension induced by output-lifting will be used to improve the assigned eigenvectors and hence the maximum number of exactly assignable elements of each eigenvector is enlarged. Furthermore, the eigenstructure will be assigned in two consecutive stages. It is assumed that at each stage, the desired eigenvalues are self-conjugate and pole-assignable. In this paper, the right s_1 ($s_1 \leq n-1$) eigenpairs are chosen to be assigned, via the right allowable subspace, in the first stage. The remaining left s_2 ($s_2 = n - s_1 \leq r$) eigenpairs are assigned, via the left allowable subspace, in the second stage. (Note that in a dual situation, the left s_1 ($s_1 \leq r - 1$) eigenpairs can be assigned in the first stage and the remaining right s_2 ($s_2 = n - s_1 \leq n - 1$) eigenpairs assigned in the second stage.)

3.1 *1st stage*

At this stage, the first s_1 eigenparis are assigned and then protected for the second stage. As described in Section 2, the first s_1 right eigenpairs satisfy

$$(A_L + B_L N_1 C_L)v_i = \lambda_i v_i \tag{16}$$

$$0 = [A_L - \lambda_i I \quad B_L]\begin{bmatrix} v_i \\ N_1 C_L v_i \end{bmatrix} \tag{17}$$

where v_i represents the ith right eigenvector and $N_1 \in \mathbb{R}^{r\times pm}$. Let

$$\text{range}\left(\begin{bmatrix} P_i \\ Q_i \end{bmatrix}\right) = \text{null}([A_L - \lambda_i I \quad B_L]) \tag{18}$$

where $P_i \in \mathbb{C}^{n\times r}$ is an orthonormal basis for the right allowable subspace used to select v_i and $Q_i \in \mathbb{C}^{r\times r}$. By establishing the design vector $f_i \in \mathbb{C}^r$ from the right allowable subspace according to

$$\begin{bmatrix} v_i \\ N_1 C_L v_i \end{bmatrix} = \begin{bmatrix} P_i \\ Q_i \end{bmatrix} f_i \tag{19}$$

The achieved eigenvector matrix $V_1 \in \mathbb{C}^{n\times s_1}$ and $S_1 \in \mathbb{C}^{r\times s_1}$ are

$$\begin{aligned} V_1 &= [v_1 \dots v_{s_1}] = [P_1 f_1, \dots, P_{s_1} f_{s_1}] \\ S_1 &= N_1 C_L V_1 = [Q_1 f_1, \dots, Q_{s_1} f_{s_1}] \end{aligned} \tag{20}$$

Due to output-lifting, $\text{rank}(C_L) = n$ and therefore $pm \geq s_1$, it follows from (20) that

$$N_1 = S_1 (C_L V_1)^\dagger + Z(I - (C_L V_1)(C_L V_1)^\dagger) \tag{21}$$

where Z is the free matrix.

Using the fact that the eigenstructure associated with the uncontrollable eigenvalues as well as those associated with the unobservable eigenvalues are invariant under output feedback (Clarke & Griffin, 2004; Fahmy & O'Reilly, 1988), in this stage, the partial eigenstructure assigned in the first stage will be protected via an output reduction. Then the protected eigenvalues will become unobservable (but controllable) corresponding to the output-reduced system.

Define a non-zero output-reduction matrix matrix $X \in \mathbb{R}^{(pm-s_1)\times pm}$ such that

$$X(C_L + D_L N_1 C_L) V_1 = 0 \tag{22}$$

where V_1 is the eigenvector matrix assigned in the first stage and X is spanned from the basis of the nullspace of $((C_L + D_L N_1 C_L) V_1)^T$.

Let $\tilde{A} = A_L + B_L N_1 C_L$, $\tilde{B} = B_L + B_L N_1 C_L$, $\tilde{C} = X(C_L + D_L N_1 C_L)$ and $\tilde{D} = X(D_L + D_L N_1 D_L)$, the output-reduced system $(\tilde{A}, \tilde{B}, \tilde{C}, \tilde{D})$ has r inputs, $pm - s_1$ outputs and s_1 unobservable (but controllable) eigenvalues corresponding to those assigned in the first stage.

3.2 *2nd stage*

The second stage aims to develop a matrix $N_2 \in \mathbb{R}^{r\times(pm-s_1)}$ such that the closed-loop system $\tilde{A} + \tilde{B} N_2 \tilde{C}$ is assigned the remaining $s_2 = n - s_1$ eigenvalues (i.e. λ_j for $j = s_1 + 1, \dots, n$) only with an associated subset of left eigenvectors. Clearly left eigenvectors are each characterized by a $pm - s_1$ dimensional left parameter vector. This raises the possibility for further improving the eigenvectors when $pm - s_1 - 1 \geq r$, which represents one of the main motivations of this paper. In this stage, the remaining left s_2 eigenpairs of $\tilde{A} + \tilde{B} N_2 \tilde{C}$ satisfy

$$w_j(\tilde{A} + \tilde{B} N_2 \tilde{C}) = w_j \lambda_j \tag{23}$$

where w_j represents the jth left eigenvector. Equation (23) is equivalent to

$$[(\tilde{A}-\lambda_j I)^T \quad \tilde{C}^T]\begin{bmatrix} w_j^T \\ (\tilde{B}N_2)^T w_j^T \end{bmatrix} = 0 \tag{24}$$

From (24), $\begin{bmatrix} w_j^T \\ (\tilde{B}N_2)^T w_j^T \end{bmatrix}$ belongs to the nullspace of $[(\tilde{A}-\lambda_j I)^T \quad \tilde{C}^T]$ which defines the left allowable subspace.

Remark 3.1: *Clearly from (24), the dimension of the left allowable subspace is $pm-s_1$ and hence the maximum number of exactly assignable elements of each eigenvector becomes $pm-s_1$. This implies another potential benefit of using output-lifting if $pm-s_1 > r$, which was not exploited by L. Chen et al. (2017). In addition, after exploiting right EA in the first step and the eigenvalue protection, the number of system outputs is reduced by s_1. Therefore, for a full state feedback system, the available number of the effective system outputs to be exploited in the second step is $n-s_1$. However for multi-stage output-lifting EA, the effective system outputs available for the second stage becomes $pm-s_1$. This shows one of the benefits of using multi-stage output-lifting EA when $pm \geq n$.*

Remark 3.2: *Equation (24) implies that even for a full state feedback system, if only a single-stage left EA was exploited, the gain matrix N_2 can only be obtained in the least square sense because the system B-matrix is not square matrix in general, and therefore the achieved closed-loop eigenvalues may not coincide with the desired eigenvalues. In this case, a single-stage full state feedback left EA using (24) is of little use. However, for multi-stage output-lifting EA, only remaining s_2 eigenvalues need to be assigned in the second stage using left EA and therefore (24) can be used to assign the remaining eigenvalues with a non-square system B-matrix. This represents another benefit of using multi-stage output-lifting EA.*

Let

$$\text{range}\left(\begin{bmatrix} L_j \\ M_j \end{bmatrix}\right) = \text{null}([\tilde{A}-\lambda_j I)^T \quad \tilde{C}^T] \tag{25}$$

where $L_j \in \mathbb{C}^{n\times(pm-s_1)}$ and $M_j \in \mathbb{C}^{(pm-s_1)\times(pm-s_1)}$. For some $g_j \in \mathbb{C}^{pm-s_1}$,

$$\begin{bmatrix} w_j^T \\ (\tilde{B}N_2)^T w_j^T \end{bmatrix} = \begin{bmatrix} L_j \\ M_j \end{bmatrix} g_j \tag{26}$$

Once the design vector g_j has been established, the matrices $W_2 \in \mathbb{C}^{s_2\times n}$ and $S_2 \in \mathbb{C}^{s_2\times(pm-s_1)}$ can be calculated through

$$\begin{aligned} W_2 &= [w_{n-r+1}^T \dots w_n^T]^T = [L_{s_1+1}g_{s_1+1}, \dots, L_n g_n]^T \\ S_2 &= W_2\tilde{B}N_2 = [M_{s_1+1}g_{s_1+1}, \dots, M_n g_n]^T \end{aligned} \tag{27}$$

Since $s_2 \leq r$, the matrix N_2 can be calculated as

$$N_2 = (W_2\tilde{B})^\dagger S_2 + (I-(W_2\tilde{B})^\dagger(W_2\tilde{B}))\tilde{Z} \tag{28}$$

where $\tilde{Z}$ represents a free matrix.

3.3 *The final gain matrix*

Proposition 3.1: *The gain matrix can be recovered from*

$$K = N(I + D_L N)^{-1} \tag{29}$$

where

$$N = N_1 + (I + N_1 D_L) N_2 X (I + D_L N_1) \tag{30}$$

where the matrices N_1 and N_2 are calculated in the stage one and the stage two respectively.

Proof. The closed-loop system matrix $(\tilde{A} + \tilde{B} N_2 \tilde{C})$, with N_2 developed in the second stage, can be written as

$$\begin{aligned} \tilde{A} + \tilde{B} N_2 \tilde{C} &= A_L + B_L N_1 C_L + (B_L + B_L N_1 D_L) N_2 X (C_L + D_L N_1 C_L) \\ &= A_L + B_L N_1 C_L + B_L (I + N_1 D_L) N_2 X (I + D_L N_1) C_L \\ &= A_L + B_L (N_1 + (I + N_1 D_L) N_2 X (I + D_L N_1)) C_L \end{aligned} \tag{31}$$

Substituting (30) into (31) yields $\tilde{A} + \tilde{B} N_2 \tilde{C} = A_L + B_L N C_L$ and therefore the matrix N is able to achieve an improved eigenstructure corresponding to the original system in (3). Then the gain matrix in (29) can be recovered from (8). □

Remark 3.3: *As argued in L. Chen et al. (2017), the term $I + D_L N$ can always be ensured to be non-singular via choosing a set of suitable desired eigenvectors (L. Chen et al., 2017).*

Remark 3.4: *With the causality constraint induced by output-lifting, any* fully-populated *gain matrix, calculated from (29), may be non-causal. As in L. Chen et al. (2017), a structural mapping can be used to relax the causality constraint.*

4. The mathematical model of Ball and Plate system

As a representative of a genuine application, a Ball and Plate system has been used for the validation and verification of various advanced multivariable control techniques (Awtar et al., 2002; Castro, Flores, Salton, & Pereira, 2014; Date, Sampei, Ishikawa, & Koga, 2004; Fan, Zhang, & Teng, 2004; Oriolo & Vendittelli, 2005; Wang, Sun, Wang, Liu, & Chen, 2014; Yuan & Zhang, 2010). The entire system model is comprised of three components, which are the Ball and Plate dynamics, the motor dynamics and the push-rod systems which establish the physical relationships between the motors and the plate. In this paper, a novel Ball and Plate system model is devised where three electric motors work cooperatively. Not only can a predefined the ball trajectory on the plate be achieved, but also the ball is maintained at a fixed height. As a consequence, the tilt axes of the plate are always underneath the ball.

The system physical structure is shown in Fig. 1 in which the rotation angles of the motor shafts are measured by the digital encoders. The tilt angles of the plate are measured by two angle sensors and a digital camera sitting above the plate measures the position and velocity of the ball. In contrast to the conventional Ball and Plate system in which only two motors are used to tilt the plate along two orthogonal axes located on the symmetric centre of the plate, here the plate is supported by three vertical pushrods which allow the tilt axis of the plate to remain underneath the rolling ball and therefore the ball will not be launched off the plate in the situation where the distance between the tilt axis and the ball is large. The control objectives are to make the ball roll along a predefined trajectory on the plate whilst maintaining the ball at a fixed datum height.

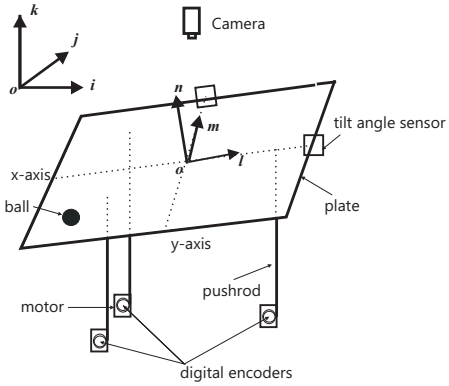

Figure 1. Physical Structure of Ball and Plate System

Consider a Ball and Plate system with the kinetic energy

$$U = \frac{1}{2}m\dot{s}^2 + \frac{1}{2}J_b\omega^2 + \frac{1}{2}J_p\omega_p^2 \tag{32}$$

and the potential energy

$$T = mgh \tag{33}$$

Then Lagrangian can be written as

$$L = \frac{1}{2}m\dot{s}^2 + \frac{1}{2}J_b\omega^2 + \frac{1}{2}J_p\omega_p^2 - mgh \tag{34}$$

By letting the plate rotate through θ followed by ϕ, a mapping between the local and inertial coordinates can be established as

$$\begin{bmatrix} o\vec{l} \\ o\vec{m} \\ o\vec{n} \end{bmatrix} = \begin{bmatrix} \cos\theta & \sin\theta\sin\phi & -\sin\theta\cos\phi \\ 0 & \cos\phi & \sin\phi \\ \sin\theta & -\cos\theta\sin\phi & \cos\theta\cos\phi \end{bmatrix} \begin{bmatrix} o\vec{i} \\ o\vec{j} \\ o\vec{k} \end{bmatrix} \tag{35}$$

where $\{o\vec{i}, o\vec{j}, o\vec{k}\}$ denotes the inertial coordinate and $\{o\vec{l}, o\vec{m}, o\vec{n}\}$ denotes the local coordinate of the plate or the coordinate of the ball relative to the plate. Suppose the coordinate of the ball relative to the plate is

$$d = x\vec{l} + y\vec{m} + r_b\vec{n} \tag{36}$$

From (35), the displacement of the ball corresponding to the plate in the inertial coordinate is

$$s = \bar{s}_1\vec{i} + \bar{s}_2\vec{j} + h\vec{k} \tag{37}$$

where

$$\begin{bmatrix} \bar{s}_1 \\ \bar{s}_2 \\ h \end{bmatrix} = \begin{bmatrix} \cos\theta & 0 & \sin\theta \\ \sin\theta\sin\phi & \cos\phi & -\cos\theta\sin\phi \\ -\sin\theta\cos\phi & \sin\phi & \cos\theta\cos\phi \end{bmatrix} \begin{bmatrix} x \\ y \\ r_b \end{bmatrix} \tag{38}$$

From (35) and (37) it follows

$$\dot{s} = (\dot{x} + r_b\dot{\theta} - y\sin\theta\dot{\phi})\vec{l} + (\dot{y} + \dot{\phi}(x\sin\theta - r_b\cos\theta))\vec{m} + (y\cos\theta\dot{\phi} - x\dot{\theta})\vec{n} \tag{39}$$

Defining an angular velocity coordinate transformation as

$$\begin{bmatrix} \tilde{p} \\ \tilde{q} \\ \tilde{r} \end{bmatrix} = \begin{bmatrix} 1 & 0 & \sin\phi \\ 0 & \cos\phi & -\sin\phi\cos\theta \\ 0 & \sin\phi & \cos\theta\cos\phi \end{bmatrix} \begin{bmatrix} \dot{\phi} \\ \dot{\theta} \\ 0 \end{bmatrix} \tag{40}$$

the angular velocity of the plate relative to the earth can be written as

$$\omega_p = \tilde{p}\vec{i} + \tilde{q}\vec{j} + \tilde{r}\vec{j} = \dot{\phi}\vec{i} + \cos\phi\dot{\theta}\vec{j} + \sin\phi\dot{\theta}\vec{k} = \cos\theta\dot{\phi}\vec{l} + \dot{\theta}\vec{m} + \sin\theta\dot{\phi}\vec{n} \tag{41}$$

The angular velocity of the ball relative to the earth is then given by

$$\omega = \omega_x\vec{l} + \omega_y\vec{m} + \omega_z\vec{n} + \omega_p = (\omega_x + \cos\theta\dot{\phi})\vec{l} + (\omega_y + \dot{\theta})\vec{m} + (\omega_z + \sin\theta\dot{\phi})\vec{n} \tag{42}$$

Substituting (38-42) into (34) yields

$$\begin{aligned} L =& \frac{1}{2}m((\dot{x} + r_b\dot{\theta} - y\sin\theta\dot{\phi})^2 + (\dot{y} + \dot{\phi}(x\sin\theta - r_b\cos\theta))^2 + (y\cos\theta\dot{\phi} - x\dot{\theta})^2) \\ &+ \frac{J_b}{2}((\omega_x + \cos\theta\dot{\phi})^2 + (\omega_y + \dot{\theta})^2 + (\omega_z + \sin\theta\dot{\phi})^2) \\ &+ \frac{J_p}{2}((\cos\theta\dot{\phi})^2 + \dot{\theta}^2 + (\sin\theta\dot{\phi})^2) - mg(-x\sin\theta\cos\phi + y\sin\phi + r_b\cos\theta\cos\phi) \end{aligned} \tag{43}$$

where

$$J_p = \frac{1}{12}m(a^2 + b^2) \quad \text{and} \quad J_b = \frac{2}{5}mr_b^2 \tag{44}$$

The Lagrangian equations with respect to x, y, ω_x and ω_y are given by

$$\frac{d}{dt}(\frac{\partial L}{\partial \dot{x}}) - \frac{\partial L}{\partial x} = f_x \qquad \frac{d}{dt}(\frac{\partial L}{\partial \dot{y}}) - \frac{\partial L}{\partial y} = f_y \tag{45}$$

$$\frac{d}{dt}(\frac{\partial L}{\partial \omega_x}) - \frac{\partial L}{\partial \psi_1} = m_{\omega_x} \qquad \frac{d}{dt}(\frac{\partial L}{\partial \omega_y}) - \frac{\partial L}{\partial \psi_2} = m_{\omega_y} \tag{46}$$

Substituting (43) into (45) and (46) yields

$$f_x = -m(-\ddot{x} - r_b\ddot{\theta} + 2\dot{y}\sin\theta\dot{\phi} + y\sin\theta\ddot{\phi} + \dot{\phi}^2 x\sin^2\theta - \sin\theta\dot{\phi}^2 r_b\cos\theta + x\dot{\theta}^2 + g\sin\theta\cos\phi) \tag{47}$$

$$f_y = m(2\dot{\phi}\sin\theta\dot{x} + 2\dot{\phi}x\cos\theta\dot{\theta} + 2\dot{\phi}r_b\sin\theta\dot{\theta} + \ddot{\phi}(x\sin\theta - r_b\cos\theta) + \ddot{y} - \dot{\phi}^2 y + g\sin\phi) \tag{48}$$

$$m_{\omega_x} = J_b(\cos\theta\ddot{\phi} - \sin\theta\dot{\theta}\dot{\phi} + \dot{\omega_x}) \tag{49}$$

$$m_{\omega_y} = J_b(\ddot{\theta} + \dot{\omega_y}) \tag{50}$$

Since the moments on the ball are produced by f_y and f_x, it follows

$$m_{\omega_x} = r_b f_y \quad \text{and} \quad m_{\omega_y} = -r_b f_x \tag{51}$$

Using the fact that $\ddot{y} = -r_b\dot{\omega_x}$ and $\ddot{x} = r_b\dot{\omega_y}$, and combining (47)-(51) yields

$$\ddot{x} = \frac{5}{7}(\sin\theta\dot{\phi}(2\dot{y} + x\sin\theta\dot{\phi} - r_b\cos\theta\dot{\phi}) + x\dot{\theta}^2 + g\sin\theta\cos\phi + y\sin\theta\ddot{\phi}) - r_b\ddot{\theta} \tag{52}$$

$$\ddot{y} = \frac{5}{7}(-2\dot{\phi}\sin\theta\dot{x} - 2\dot{\phi}x\cos\theta\dot{\theta} - x\sin\theta\ddot{\phi} - \frac{12}{5}r_b\dot{\phi}\sin\theta\dot{\theta} + \dot{\phi}^2 y - g\sin\phi) + r_b\cos\theta\ddot{\phi} \tag{53}$$

As defined in Fig. 2, (X_1, Y_1, Z_1), (X_2, Y_2, Z_2) and (X_3, Y_3, Z_3) represent the coordinates of three points connected to the pushrods. So, by inspecting Figure 3,

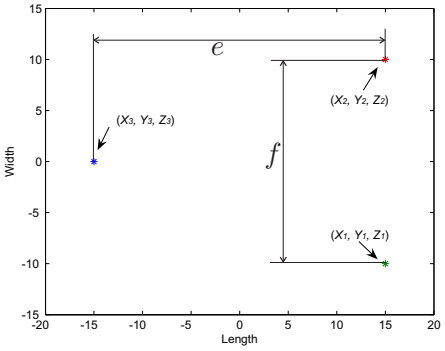

Figure 2. Surface of the Plate

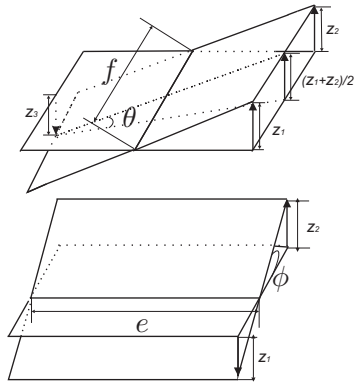

Figure 3. Relationship Between Tilting Angles of Plate and Displacements of Pushrods

$$\theta = \arcsin\frac{Z_3 - \frac{Z_1+Z_2}{2}}{e} \quad \text{and} \quad \phi = \arcsin\frac{Z_2 - Z_1}{f} \tag{54}$$

and $\dot{\theta}$, $\dot{\phi}$, $\ddot{\theta}$ and $\ddot{\phi}$, derived from (54), are given by

$$\dot{\theta} = \frac{2\dot{Z}_3 - \dot{Z}_1 - \dot{Z}_2}{2e\cos\theta} \quad \dot{\phi} = \frac{\dot{Z}_2 - \dot{Z}_1}{f\cos\phi} \tag{55}$$

$$\ddot{\theta} = \frac{2\ddot{Z}_3 - \ddot{Z}_1 - \ddot{Z}_2}{2e\cos\theta} + \frac{(\dot{Z}_3 - \frac{\dot{Z}_1+\dot{Z}_2}{2})^2(Z_3 - \frac{Z_1+Z_2}{2})}{e^3(\cos^2\theta)^{\frac{3}{2}}} \tag{56}$$

$$\ddot{\phi} = \frac{\ddot{Z}_2 - \ddot{Z}_1}{f\cos\phi} + \frac{(\dot{Z}_2 - \dot{Z}_1)^2(Z_2 - Z_1)}{f^3(\cos^2\phi)^{\frac{3}{2}}} \tag{57}$$

where

$$\cos\theta = \sqrt{1 - (\frac{Z_3 - \frac{Z_1+Z_2}{2}}{e})^2} \quad \text{and} \quad \cos\phi = \sqrt{1 - (\frac{Z_2 - Z_1}{f})^2}$$

As shown in Fig. 4, the motor-pushrod mechanism ensures three push-rods to move vertically. The pushrod is always under compression due to the existence of the spring and therefore any backlash in the motor gears is eliminated. The length of the rod is chosen to be at least ten times that of

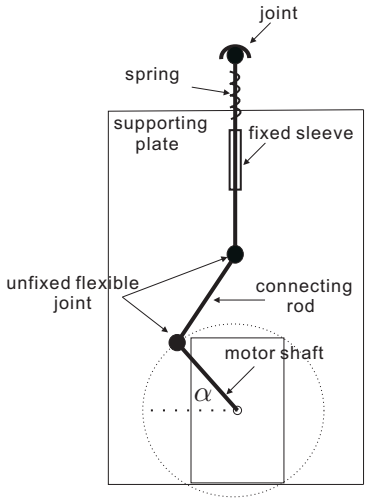

Figure 4. Motor-Pushrod Mechanism

the motor shaft so that the angle between the connecting rod and the vertical line remains small. Using the small-angle approximation, the vertical displacement of the ith push-rod is given by

$$Z_i = l \sin\alpha_i \quad \forall i = 1:3 \tag{58}$$

where l is the length of the motor shaft, α_i is the rotation angle of the ith motor shaft.
Using the plate surface equation

$$\begin{vmatrix} x - X_1 & y - Y_1 & h - Z_1 \\ X_2 - X_1 & Y_2 - Y_1 & Z_2 - Z_1 \\ X_3 - X_1 & Y_3 - Y_1 & Z_3 - Z_1 \end{vmatrix} = 0 \tag{59}$$

and substituting (58) into (59), $\ddot{h}$ can be expressed using x, y, $\dot{x}$, $\dot{y}$, $\ddot{x}$, $\ddot{y}$, α_i, $\dot{\alpha}_i$ and $\ddot{\alpha}_i$ $(i = 1:3)$.

Here in this example, the angular accelerations of the plane (i.e. $\ddot{\theta}$ and $\ddot{\phi}$ from (56) and (57)) and the accelerations of the three pushrods (i.e. $\ddot{\alpha}_i,\ i = 1:3$) cannot be measured straightforwardly. Based upon Kirchhoff's law, the equation that describes the electric circuit of each armature is

$$L_a \frac{dI_i}{dt} + R_m I_i = \bar{V}_i - K_e \dot{\alpha}_i \quad \forall i = 1:3 \tag{60}$$

Clearly from (60), a relationship between current flow into the motor and the angular velocity of the rotor is established. Using the torque balance equation, the angular acceleration of the rotor

can be written as

$$\ddot{\alpha_i} = \frac{K_t(\bar{V}_i - L_a\dot{I}_i) - (K_tK_e + R_m\tilde{b})\dot{\alpha}}{J_mR_m} \quad \forall = 1:3 \tag{61}$$

Using the appropriate equations derived above, the full nonlinear Ball and Plate system model can be built. The values of physical parameters used subsequently in this paper are listed in Table 1.

Table 1. Model Parameters

Parameter	Value	Parameter	Value
e	$0.3(m)$	$\tilde{b}$	$1.5297(Nm/(rad/s))$
f	$0.2(m)$	K_t	3 (v/rpm)
r_b	$0.0175(m)$	J_m	$0.4(kgm^2)$
(X_1, Y_1)	$(0.15, -0.1)(m)$	K_e	$4.77(v/rpm)$
(X_2, Y_2)	$(0.15, 0.1)(m)$	R_m	$4.7(\Omega)$
(X_3, Y_3)	$(-0.15, 0)(m)$	L_a	$0.4(H)$
a	$0.4(m)$	b	$0.3(m)$
l	$0.05(m)$	g	$9.81(Nm/s^2)$

5. Determination of the Desired Eigenstructure

5.1 *Selecting the Desired Eigenvector*

This section demonstrates how to develop a set of ideal eigenstructure via the analysis of the physical characteristics of Ball and Plate system. Let the model developed in the earlier section be trimmed and linearised round the geometric centre of the ball and the plate, full system states can be written as

$$x_{full} = [x \;\; \dot{x} \;\; y \;\; \dot{y} \;\; \alpha_1 \;\; \alpha_2 \;\; \alpha_3 \;\; \dot{\alpha_1} \;\; \dot{\alpha_2} \;\; \dot{\alpha_3} \;\; I_1 \;\; I_2 \;\; I_3]^T \tag{62}$$

Due to the fast dynamics of the motor armature currents, their states I_1, I_2 and I_3 can be eliminated from (62). So,

$$x_r = \begin{bmatrix} x & \dot{x} & y & \dot{y} & \alpha_1 & \alpha_2 & \alpha_3 & \dot{\alpha}_1 & \dot{\alpha}_2 & \dot{\alpha}_3 \end{bmatrix}^T \tag{63}$$

Define a coordinate transformation $\tilde{x} \mapsto Tx_r$ in terms of the mathematical model developed in Section 4, and in the new coordinate, system states are given by

$$\tilde{x} = \begin{bmatrix} x & \dot{x} & y & \dot{y} & \phi & \dot{\phi} & \theta & \dot{\theta} & h & \dot{h} \end{bmatrix}^T \tag{64}$$

and system inputs $\tilde{u}$ and outputs $\tilde{y}$ are selected as

$$\begin{aligned} \tilde{u} &= \begin{bmatrix} \bar{V}_1 & \bar{V}_2 & \bar{V}_3 \end{bmatrix}^T \\ \tilde{y} &= \begin{bmatrix} x & y & \dot{x} & \dot{y} & \phi & \theta & h \end{bmatrix}^T \end{aligned} \tag{65}$$

where $\bar{V}_i$ is from (61). The state space matrices associated with the new coordination system are given in Appendix A.

Remark 5.1: *In this special three-motor Ball and Plate system, it is unrealistic the derive the desired eigenstructure in terms of system states in (63). This is because states x, y, $\dot{x}$ and $\dot{y}$ are coupled with states α_i and $\dot{\alpha}_i$. In the new coordinate system, the system states in $\tilde{x}$ can be divided into three groups: (x, $\dot{x}$, θ, $\dot{\theta}$), (y, $\dot{y}$, ϕ, $\dot{\phi}$) and (h, $\dot{h}$) and each group is decoupled from the rest.*

In this paper, the transfer function approach is used to preserve the integral relationships between system states. For the subsystem corresponding to the first group of system states, eigenvalues will be assigned as follows: one complex pair of poles $(\lambda_x, \bar{\lambda_x})$ to determine the second-order response of the position and velocity of the ball, and one complex pair of poles $(\lambda_\theta, \bar{\lambda_\theta})$ to determine the second-order response of the angular position and angular velocity of the plate. The responses of the position of the ball and the angle of the plate are related to the velocity of the ball and the angular velocity of the plate through integration. Furthermore, based upon the kinematics developed in the earlier section, the mode corresponding to the ball dynamics is not visible in the plate dynamics but the mode corresponding to the plate dynamics *is* visible in the ball dynamics. Therefore the set of transfer functions can be written as

$$\begin{aligned}
\frac{x}{u_1} &= \frac{1}{(s+\lambda_x)(s+\bar{\lambda_x})(s+\lambda_\theta)(s+\bar{\lambda_\theta})} \\
\frac{\dot{x}}{u_1} &= \frac{s}{(s+\lambda_x)(s+\bar{\lambda_x})(s+\lambda_\theta)(s+\bar{\lambda_\theta})} \\
\frac{\theta}{u_1} &= \frac{1}{(s+\lambda_\theta)(s+\bar{\lambda_\theta})} \\
\frac{\dot{\theta}}{u_1} &= \frac{s}{(s+\lambda_\theta)(s+\bar{\lambda_\theta})}
\end{aligned} \tag{66}$$

where u_1 denotes the input excitation associated with the subsystem (x, $\dot{x}$, θ, $\dot{\theta}$). Let the fourth-order subsystem have an input matrix $B_s = [0\ \ 0\ \ 0\ \ 1]^T$, an output matrix $C_s = I_4$, a modal matrix denoted by Λ_s, and let the left and right eigenvectors be denoted by W_s and V_s, respectively. The transfer function of the subsystem can be written as

$$G_s(s) = C_s V_s (sI - \Lambda_s)^{-1} W_s B_s \tag{67}$$

By defining r_i as elements of $C_s V_s$ and t_i as elements of $W_s B_s$, (67) can be expanded as follows:

$$\begin{bmatrix} x \\ \dot{x} \\ \theta \\ \dot{\theta} \end{bmatrix} = \begin{bmatrix} \bar{r_1} & r_1 & \bar{r_5} & r_5 \\ \bar{r_2} & r_2 & \bar{r_6} & r_6 \\ \bar{r_3} & r_3 & 0 & 0 \\ \bar{r_4} & r_4 & 0 & 0 \end{bmatrix} \begin{bmatrix} \frac{1}{s+\lambda_\theta} & 0 & 0 & 0 \\ 0 & \frac{1}{s+\lambda_\theta} & 0 & 0 \\ 0 & 0 & \frac{1}{s+\lambda_x} & 0 \\ 0 & 0 & 0 & \frac{1}{s+\bar{\lambda_x}} \end{bmatrix} \begin{bmatrix} \bar{t_1} \\ t_1 \\ \bar{t_2} \\ t_2 \end{bmatrix} u_1 \tag{68}$$

In (68), null elements appear in $C_s V_s$ because the mode λ_x is not visible in θ and $\dot{\theta}$. From (68),

$$\begin{aligned}
\frac{x}{u_1} &= \frac{\bar{r_1}\bar{t_1}}{s+\lambda_\theta} + \frac{r_1 t_1}{s+\bar{\lambda_\theta}} + \frac{\bar{r_5}\bar{t_2}}{s+\lambda_x} + \frac{r_5 t_2}{s+\bar{\lambda_x}} \\
\frac{\dot{x}}{u_1} &= \frac{\bar{r_2}\bar{t_1}}{s+\lambda_\theta} + \frac{r_2 t_1}{s+\bar{\lambda_\theta}} + \frac{\bar{r_6}\bar{t_2}}{s+\lambda_x} + \frac{r_6 t_2}{s+\bar{\lambda_x}} \\
\frac{\theta}{u_1} &= \frac{\bar{r_3}\bar{t_1}}{s+\lambda_\theta} + \frac{r_3 t_1}{s+\bar{\lambda_\theta}} \\
\frac{\dot{\theta}}{u_1} &= \frac{\bar{r_4}\bar{t_1}}{s+\lambda_\theta} + \frac{r_4 t_1}{s+\bar{\lambda_\theta}}
\end{aligned} \tag{69}$$

Equating coefficients with the numerators of the ideal transfer functions, the eigenvector elements r_i $(i = 1, \ldots, 6)$, t_1 and t_2 satisfy

$$\begin{aligned}
\frac{x}{u_1} \quad s^3 : 0 =& \bar{r_1}\bar{t_1} + r_1 t_1 + \bar{r_5}\bar{t_2} + r_5 t_2 && (70)\\
s^2 : 0 =& \bar{r_1}\bar{t_1}(\lambda_x + \bar{\lambda_x} + \bar{\lambda_\theta}) + r_1 t_1(\lambda_\theta + \lambda_x + \bar{\lambda_x}) + \bar{r_5}\bar{t_2}(\lambda_\theta + \bar{\lambda_x} + \bar{\lambda_\theta}) \\
& + r_5 t_2(\lambda_\theta + \lambda_x + \bar{\lambda_\theta}) && (71)\\
s^1 : 0 =& \bar{r_1}\bar{t_1}(\bar{\lambda_\theta}\lambda_x + \bar{\lambda_\theta}\bar{\lambda_x} + \lambda_x\bar{\lambda_x}) + r_1 t_1(\lambda_\theta\lambda_x + \lambda_\theta\bar{\lambda_x} + \bar{\lambda_x}\lambda_x) \\
& + \bar{r_5}\bar{t_2}(\lambda_\theta\bar{\lambda_\theta} + \lambda_\theta\bar{\lambda_x} + \bar{\lambda_\theta}\bar{\lambda_x}) + r_5 t_2(\lambda_\theta\bar{\lambda_\theta} + \lambda_\theta\lambda_x + \bar{\lambda_\theta}\lambda_x) && (72)\\
s^0 : 0 \neq& \bar{r_1}\bar{t_1}\bar{\lambda_\theta}\lambda_x\bar{\lambda_x} + r_1 t_1\lambda_\theta\lambda_x\bar{\lambda_x} + \bar{r_5}\bar{t_2}\lambda_\theta\bar{\lambda_\theta}\bar{\lambda_x} + r_5 t_2\lambda_\theta\bar{\lambda_\theta}\lambda_x && (73)\\
\frac{\dot{x}}{u_1} \quad s^3 : 0 =& \bar{r_2}\bar{t_1} + r_2 t_1 + \bar{r_6}\bar{t_2} + r_6 t_2 && (74)\\
s^2 : 0 =& \bar{r_2}\bar{t_1}(\lambda_x + \bar{\lambda_x} + \bar{\lambda_\theta}) + r_2 t_1(\lambda_\theta + \lambda_x + \bar{\lambda_x}) + \bar{r_6}\bar{t_2}(\lambda_\theta + \bar{\lambda_x} + \bar{\lambda_\theta}) \\
& + r_6 t_2(\lambda_\theta + \lambda_x + \bar{\lambda_\theta}) && (75)\\
s^1 : 0 \neq& \bar{r_2}\bar{t_1}(\bar{\lambda_\theta}\lambda_x + \bar{\lambda_\theta}\bar{\lambda_x} + \lambda_x\bar{\lambda_x}) + r_2 t_1(\lambda_\theta\lambda_x + \lambda_\theta\bar{\lambda_x} + \bar{\lambda_x}\lambda_x) \\
& + \bar{r_6}\bar{t_2}(\lambda_\theta\bar{\lambda_\theta} + \lambda_\theta\bar{\lambda_x} + \bar{\lambda_\theta}\bar{\lambda_x}) + r_6 t_2(\lambda_\theta\bar{\lambda_\theta} + \lambda_\theta\lambda_x + \bar{\lambda_\theta}\lambda_x) && (76)\\
s^0 : 0 =& \bar{r_2}\bar{t_1}\bar{\lambda_\theta}\lambda_x\bar{\lambda_x} + r_2 t_1\lambda_\theta\lambda_x\bar{\lambda_x} + \bar{r_6}\bar{t_2}\lambda_\theta\bar{\lambda_\theta}\bar{\lambda_x} + r_6 t_2\lambda_\theta\bar{\lambda_\theta}\lambda_x && (77)\\
\frac{\theta}{u_1} \quad s^1 : 0 =& \bar{r_3}\bar{t_1} + r_3 t_1 && (78)\\
s^0 : 0 \neq& \bar{r_3}\bar{t_1}\bar{\lambda_\theta} + r_3 t_1\lambda_\theta && (79)\\
\frac{\dot{\theta}}{u_1} \quad s^1 : 0 \neq& \bar{r_4}\bar{t_1} + r_4 t_1 && (80)\\
s^0 : 0 =& \bar{r_4}\bar{t_1}\bar{\lambda_\theta} + r_4 t_1\lambda_\theta && (81)
\end{aligned}$$

Note that not all of the above eigenvector elements can be arbitrarily assigned, and the left and right eigenvectors must satisfy

$$I_4 = W_s V_s \tag{82}$$

Equation (82) can be converted into the following constraints on $r_i (i = 1, \ldots, 6)$, t_1 and t_2 as

$$[0 \;\; 0 \;\; 0 \;\; 1]^T = C_s V_s W_s B_s \tag{83}$$

$$\begin{bmatrix} 0 \\ 0 \\ 0 \\ 1 \end{bmatrix} = \begin{bmatrix} \bar{r_1}\bar{t_1} + r_1 t_1 + \bar{r_5}\bar{t_2} + r_5 t_2 \\ \bar{r_2}\bar{t_1} + r_2 t_1 + \bar{r_6}\bar{t_2} + r_6 t_2 \\ \bar{r_3}\bar{t_1} + r_3 t_1 \\ \bar{r_4}\bar{t_1} + r_4 t_1 \end{bmatrix} \tag{84}$$

Examination of (84) shows that the constraints in (70), (74) and (78) are inherently satisfied. To satisfy (81),

$$r_4 = \frac{r_3}{\lambda_\theta} \quad \text{and} \quad \bar{r_4} = \frac{\bar{r_3}}{\bar{\lambda_\theta}} \tag{85}$$

which will satisfy equation (78). Substituting (85) into (71) and (72) to eliminate $\bar{r_5}\bar{r_2}$ yields

$$0 = \bar{r_1}\bar{t_1}\lambda_x + r_1t_1\lambda_x + r_5t_2\lambda_x - \bar{r_1}\bar{t_1}\lambda_\theta - r_1t_1\bar{\lambda_\theta} - r_5t_2\bar{\lambda_x} \tag{86}$$

and

$$\begin{aligned} 0 =& \bar{r_1}\bar{t_1}(\bar{\lambda_\theta}\lambda_x + \lambda_x\bar{\lambda_x} - \lambda_\theta\bar{\lambda_\theta} - \lambda_\theta\bar{\lambda_\theta}) + r_1t_1(\lambda_\theta\lambda_x + \lambda_x\bar{\lambda_x} - \lambda_\theta\bar{\lambda_\theta} - \bar{\lambda_\theta}\bar{\lambda_x}) \\ &+ r_5r_2(\lambda_\theta\lambda_x + \bar{\lambda_\theta}\lambda_x - \lambda_\theta\bar{\lambda_x} - \bar{\lambda_\theta}\bar{\lambda_x}) \end{aligned} \tag{87}$$

Substituting (86) into (87) to eliminate r_5r_2 yields

$$0 = \bar{r_1}\bar{t_1}(\lambda_x\bar{\lambda_x} - \lambda_\theta\bar{\lambda_x} - \lambda_x\lambda_\theta + \lambda_\theta\lambda_\theta) + r_1t_1(\lambda_x\bar{\lambda_x} - \bar{\lambda_\theta}\bar{\lambda_x} - \lambda_x\bar{\lambda_\theta} + \bar{\lambda_\theta}\bar{\lambda_\theta}) \tag{88}$$

From (78) it follows that

$$\begin{aligned} r_1 &= \frac{r_3}{\lambda_x\bar{\lambda_x} - \bar{\lambda_\theta}\bar{\lambda_x} - \bar{\lambda_\theta}\lambda_x + \bar{\lambda_\theta}^2} \\ \bar{r_1} &= \frac{\bar{r_3}}{\lambda_x\bar{\lambda_x} - \lambda_\theta\bar{\lambda_x} - \lambda_\theta\lambda_x + \lambda_\theta^2} \end{aligned} \tag{89}$$

Substituting (74) into (75) and (77) to eliminate $\bar{r_6}\bar{t_2}$ yields

$$0 = \bar{r_2}\bar{t_1}\lambda_x + r_2t_1\lambda_x + r_6t_2\lambda_x - \bar{r_2}\bar{t_1}\lambda_\theta - r_2t_1\bar{\lambda_\theta} - r_6t_2\bar{\lambda_x} \tag{90}$$

and

$$0 = \bar{r_2}\bar{t_1}(\bar{\lambda_\theta}\lambda_x\bar{\lambda_x} - \lambda_\theta\bar{\lambda_\theta}\bar{\lambda_x}) + r_2t_1(\lambda_\theta\lambda_x\bar{\lambda_x} - \lambda_\theta\bar{\lambda_\theta}\bar{\lambda_x}) + r_6r_2(\lambda_\theta\bar{\lambda_\theta}\lambda_x - \lambda_\theta\bar{\lambda_\theta}\bar{\lambda_x}) \tag{91}$$

Substituting (90) into (91) to eliminate r_6r_2 yields

$$0 = \bar{r_2}\bar{r_1}(\bar{\lambda_\theta}\lambda_x\bar{\lambda_x} - \lambda_\theta\bar{\lambda_\theta}\bar{\lambda_x} - \lambda_\theta\bar{\lambda_\theta}\lambda_x + \lambda_\theta^2\bar{\lambda_\theta}) + r_2r_1(\lambda_\theta\lambda_x\bar{\lambda_x} - \lambda_\theta\bar{\lambda_\theta}\bar{\lambda_x} - \lambda_\theta\bar{\lambda_\theta}\lambda_x + \lambda_\theta\bar{\lambda_\theta}^2) \tag{92}$$

Comparing (78) and (92), r_2 can be expressed as

$$\begin{aligned} r_2 &= \frac{r_3}{\lambda_\theta\lambda_x\bar{\lambda_x} - \lambda_\theta\bar{\lambda_\theta}\bar{\lambda_x} - \lambda_\theta\bar{\lambda_\theta}\lambda_x + \lambda_\theta\bar{\lambda_\theta}^2} \\ \bar{r_2} &= \frac{\bar{r_3}}{\bar{\lambda_\theta}\lambda_x\bar{\lambda_x} - \lambda_\theta\bar{\lambda_\theta}\bar{\lambda_x} - \lambda_\theta\bar{\lambda_\theta}\lambda_x + \lambda_\theta^2\bar{\lambda_\theta}} \end{aligned} \tag{93}$$

Now substituting (70) into (71) and (72) respectively to eliminate $\bar{r_1}\bar{t_1}$ yields

$$\begin{aligned} 0 =& r_1t_1(\lambda_\theta\lambda_x + \lambda_\theta\bar{\lambda_x} - \bar{\lambda_\theta}\lambda_x - \bar{\lambda_\theta}\bar{\lambda_x}) + \bar{r_5}\bar{r_2}(\lambda_\theta\bar{\lambda_\theta} + \lambda_\theta\bar{\lambda_x} - \bar{\lambda_\theta}\lambda_x - \lambda_x\bar{\lambda_x}) \\ &+ r_5r_2(\lambda_\theta\bar{\lambda_\theta} + \lambda_\theta\lambda_x - \bar{\lambda_\theta}\bar{\lambda_x} - \lambda_x\bar{\lambda_x}) \end{aligned} \tag{94}$$

and

$$0 = r_1t_1(\lambda_\theta - \bar{\lambda_\theta}) + r_5t_2(\lambda_\theta - \bar{\lambda_x}) + \bar{r_5}\bar{r_2}(\lambda_\theta - \lambda_x) \tag{95}$$

After combining (94) and (95) to eliminate $r_1 t_1$, it follows that

$$0 = \bar{r_5}\bar{t_2}(\lambda_\theta\bar{\lambda_\theta} - \bar{\lambda_\theta}\lambda_x - \lambda_\theta\lambda_x + \lambda_x^2) + r_5 r_2(\lambda_\theta\bar{\lambda_\theta} - \bar{\lambda_\theta}\bar{\lambda_x} - \lambda_\theta\bar{\lambda_x} + \bar{\lambda_x}^2) \tag{96}$$

Similarly, (74) is substituted into (75) and (77) to eliminate $\bar{r_2}\bar{t_1}$, which yields

$$0 = r_2 t_1(\lambda_\theta\lambda_x\bar{\lambda_x} - \bar{\lambda_\theta}\lambda_x\bar{\lambda_x}) + \bar{r_6}\bar{r_2}(\lambda_\theta\bar{\lambda_\theta}\bar{\lambda_x} - \bar{\lambda_\theta}\lambda_x\bar{\lambda_x}) + r_6 r_2(\lambda_\theta\bar{\lambda_\theta}\lambda_x - \bar{\lambda_\theta}\lambda_x\bar{\lambda_x}) \tag{97}$$

and

$$0 = r_2 t_1(\lambda_\theta - \bar{\lambda_\theta}) + \bar{r_6}\bar{t_2}(\lambda_\theta - \lambda_x) + r_6 r_2(\lambda_\theta - \bar{\lambda_x}) \tag{98}$$

Combining (97) and (98) to eliminate $r_2 t_1$:

$$0 = \bar{r_6}\bar{t_2}(\lambda_\theta\bar{\lambda_\theta}\bar{\lambda_x} - \bar{\lambda_\theta}\lambda_x\bar{\lambda_x} - \lambda_x\bar{\lambda_x}\lambda_\theta + \lambda_x^2\bar{\lambda_x}) + r_6 r_2(\lambda_\theta\bar{\lambda_\theta}\lambda_x - \bar{\lambda_\theta}\lambda_x\bar{\lambda_x} - \lambda_x\bar{\lambda_x}\lambda_\theta + \lambda_x\bar{\lambda_x}^2) \tag{99}$$

From (96) and (99), r_6 and $\bar{r_6}$ can be expressed by r_5 and $\bar{r_5}$ respectively:

$$\begin{aligned} r_6 &= \frac{r_5(\lambda_\theta\bar{\lambda_\theta} - \bar{\lambda_\theta}\bar{\lambda_x} - \lambda_\theta\bar{\lambda_x} + \bar{\lambda_x}^2)}{\lambda_\theta\bar{\lambda_\theta}\lambda_x - \bar{\lambda_\theta}\lambda_x\bar{\lambda_x} - \lambda_x\bar{\lambda_x}\lambda_\theta + \lambda_x\bar{\lambda_x}^2} \\ \bar{r_6} &= \frac{\bar{r_5}(\lambda_\theta\bar{\lambda_\theta} - \bar{\lambda_\theta}\lambda_x - \lambda_\theta\lambda_x + \lambda_x^2)}{\lambda_\theta\bar{\lambda_\theta}\bar{\lambda_x} - \bar{\lambda_\theta}\lambda_x\bar{\lambda_x} - \lambda_x\bar{\lambda_x}\lambda_\theta + \lambda_x^2\bar{\lambda_x}} \end{aligned} \tag{100}$$

For the second group of states $(y, \dot{y}, \theta, \dot{\theta})$, the desired closed-loop eigenvectors can be developed simply by replacing λ_x,λ_θ in (85-100) with λ_y, λ_ϕ.

For the third group of states, $\dot{h}$ and h, let the second-order subsystem have an input matrix $[0 \quad 1]^T$ and define r_7 and r_8 as the elements of the corresponding eigenvectors. The subsystem transfer function matrix can then be expressed as

$$\begin{bmatrix} h \\ \dot{h} \end{bmatrix} = \begin{bmatrix} \bar{r_7} & r_7 \\ \bar{r_8} & r_8 \end{bmatrix} \begin{bmatrix} \frac{1}{s+\lambda_h} & 0 \\ 0 & \frac{1}{s+\bar{\lambda_h}} \end{bmatrix} \begin{bmatrix} \bar{t_3} \\ t_3 \end{bmatrix} u_3 \tag{101}$$

where u_3 denotes the input excitation associated with the subsystem (h, $\dot{h}$). From (101),

$$\begin{aligned} \frac{h}{u_3} &= \frac{\bar{r_7}\bar{t_3}}{s+\lambda_h} + \frac{r_7 t_3}{s+\bar{\lambda_h}} \\ \frac{\dot{h}}{u_3} &= \frac{\bar{r_8}\bar{t_3}}{s+\lambda_h} + \frac{r_8 t_3}{s+\bar{\lambda_h}} \end{aligned} \tag{102}$$

After equating coefficients with the numerators of the ideal transfer functions, the eigenvector elements r_7, r_8, $\bar{t_3}$ and t_3 satisfy

$$\frac{h}{u_3} \quad s^1 : 0 = \bar{r_7}\bar{t_3} + r_7 t_3 \tag{103}$$

$$s^0 : 0 \neq \bar{r_7}\bar{t_3}\bar{\lambda_h} + r_7 t_3\lambda_h \tag{104}$$

$$\frac{\dot{h}}{u_3} \quad s^1 : 0 \neq \bar{r_8}\bar{t_3} + r_8 t_3 \tag{105}$$

$$s^0 : 0 = \bar{r_8}\bar{t_3}\bar{\lambda_h} + r_8 t_3\lambda_h \tag{106}$$

Comparing (103) and (106) yields

$$r_8 = \frac{r_7}{\lambda_h} \quad \text{and} \quad \bar{r_8} = \frac{\bar{r_7}}{\bar{\lambda_h}} \tag{107}$$

Since only the directions of eigenvectors are crucial for the design purpose, r_3, r_5 and r_7 are normalized to unity for convenience. After combining (85), (89), (93), (100) and (107), the complete set of ideal closed-loop eigenvectors for the system, which is consistent with the original requirements, is given by

$$\begin{bmatrix} x \\ \dot{x} \\ y \\ \dot{y} \\ \phi \\ \dot{\phi} \\ \theta \\ \dot{\theta} \\ h \\ \dot{h} \end{bmatrix} \sim \begin{bmatrix} 1 & 1 & 0 & 0 & 0 & 0 & \bar{c_6} & c_6 & 0 & 0 \\ \bar{c_1} & c_1 & 0 & 0 & 0 & 0 & \bar{c_7} & c_7 & 0 & 0 \\ 0 & 0 & 1 & 1 & \bar{c_3} & c_3 & 0 & 0 & 0 & 0 \\ 0 & 0 & \bar{c_2} & c_2 & \bar{c_4} & c_4 & 0 & 0 & 0 & 0 \\ 0 & 0 & 0 & 0 & 1 & 1 & 0 & 0 & 0 & 0 \\ 0 & 0 & 0 & 0 & \bar{c_5} & c_5 & 0 & 0 & 0 & 0 \\ 0 & 0 & 0 & 0 & 0 & 0 & 1 & 1 & 0 & 0 \\ 0 & 0 & 0 & 0 & 0 & 0 & \bar{c_8} & c_8 & 0 & 0 \\ 0 & 0 & 0 & 0 & 0 & 0 & 0 & 0 & 1 & 1 \\ 0 & 0 & 0 & 0 & 0 & 0 & 0 & 0 & \bar{c_9} & c_9 \end{bmatrix} \tag{108}$$

where $\sim$ denotes correspondence between states and matrix rows and

$$\begin{aligned} c_1 &= \frac{\lambda_\theta \bar{\lambda_\theta} - \bar{\lambda_\theta}\bar{\lambda_x} - \lambda_\theta \bar{\lambda_x} + \bar{\lambda_x}^2}{\lambda_\theta \bar{\lambda_\theta} \lambda_x - \bar{\lambda_\theta}\lambda_x \bar{\lambda_x} - \lambda_x \bar{\lambda_x} \lambda_\theta + \lambda_x \bar{\lambda_x}^2} \\ c_2 &= \frac{\lambda_\phi \bar{\lambda_\phi} - \bar{\lambda_\phi}\bar{\lambda_y} - \lambda_\phi \bar{\lambda_y} + \bar{\lambda_y}^2}{\lambda_\phi \bar{\lambda_\phi} \lambda_y - \bar{\lambda_\phi}\lambda_y \bar{\lambda_y} - \lambda_y \bar{\lambda_y} \lambda_\phi + \lambda_y \bar{\lambda_y}^2} \\ c_3 &= \frac{1}{\lambda_y \bar{\lambda_y} - \bar{\lambda_\phi}\bar{\lambda_y} - \bar{\lambda_\phi}\lambda_y + \bar{\lambda_\phi}^2} \\ c_4 &= \frac{1}{\lambda_\phi \lambda_y \bar{\lambda_y} - \lambda_\phi \bar{\lambda_\phi} \bar{\lambda_y} - \lambda_\phi \bar{\lambda_\phi} \lambda_y + \lambda_\phi \bar{\lambda_\phi}^2} \\ c_5 &= \frac{1}{\lambda_\phi} \quad c_6 = \frac{1}{\lambda_x \bar{\lambda_x} - \bar{\lambda_\theta}\bar{\lambda_x} - \bar{\lambda_\theta}\lambda_x + \bar{\lambda_\theta}^2} \\ c_7 &= \frac{1}{\lambda_\theta \lambda_x \bar{\lambda_x} - \lambda_\theta \bar{\lambda_\theta} \bar{\lambda_x} - \lambda_\theta \bar{\lambda_\theta} \lambda_x + \lambda_\theta \bar{\lambda_\theta}^2} \\ c_8 &= \frac{1}{\lambda_\theta} \quad c_9 = \frac{1}{\lambda_h} \end{aligned} \tag{109}$$

5.2 *Defining Ideal Eigenvalues*

The damping ratios of all system eigenvalues/modes are assumed to be 0.8. In the Ball and Plate system, both the ball and the plate dynamics are slower than those of the three motors, and the settling times of the modes corresponding to the tilt angles of the plate are assumed to be faster than the mode associated with the ball position. By increasing the settling time of the tilt angles of the plate, the control effort is reduced and the movement of the plate becomes smoother. Furthermore, in order to maintain the ball at a fixed height, the mode associated with the ball height is assumed to be faster than those associated with the tilt angles of the plate. The set of

desired eigenvalues in continuous-time is

$$\begin{aligned}
\{\lambda_x, \bar{\lambda_x}\} &= -0.8 \pm 0.6i \\
\{\lambda_y, \bar{\lambda_y}\} &= -0.6 \pm 0.45i \\
\{\lambda_\phi, \bar{\lambda_\phi}\} &= -5 \pm 4i \\
\{\lambda_\theta, \bar{\lambda_\theta}\} &= -4.5 \pm 3.6i \\
\{\lambda_h, \bar{\lambda_h}\} &= -15 \pm 12i
\end{aligned} \tag{110}$$

6. Application of Multistage Output-Lifting Eigenstructure Assignment

The Ball and Plate system is a typical multirate output feedback control system. Sensors and actuators around the system operating at different sampled rates. The camera samples the ball position and velocity every $40ms$. The tilt angles of the plate are measured by digital encoders which operate every $10ms$. The height of the ball is calculated using hardware logic with the sampling interval chosen to be $10ms$. The DC motors are driven by PWM signals with a frame rate of $40ms$. From (64-65), $m = 7$, $n = 10$, $r = 3$. It is not straightforward to fully assign a desired eigenstructure using a traditional output feedback EA framework because $m + r = n$. So, let the main sampling period be $40ms$ and the base sampling period be $10ms$. Then the desired discrete-time eigenvalues associated with $\tilde{x}$, discretized using the main sampling period $40ms$, are

$$\Lambda_d = diag([\lambda_{dx} \quad \bar{\lambda_{dx}} \quad \lambda_{dy} \quad \bar{\lambda_{dy}} \quad \lambda_{d\phi} \quad \bar{\lambda_{d\phi}} \quad \lambda_{d\theta} \quad \bar{\lambda_{d\theta}} \quad \lambda_{dh} \quad \bar{\lambda_{dh}}]) \tag{111}$$

where

$$\begin{aligned}
\{\lambda_{dx}, \bar{\lambda_{dx}}\} &= 0.9682 \pm 0.0232i \\
\{\lambda_{dy}, \bar{\lambda_{dy}}\} &= 0.9761 \pm 0.0176i \\
\{\lambda_{d\phi}, \bar{\lambda_{d\phi}}\} &= 0.8083 \pm 0.1304i \\
\{\lambda_{d\theta}, \bar{\lambda_{d\theta}}\} &= 0.8266 \pm 0.1199i \\
\{\lambda_{dh}, \bar{\lambda_{dh}}\} &= 0.4868 \pm 0.2534i
\end{aligned} \tag{112}$$

The desired left and right eigenvectors can be calculated by substituting desired continuous-time eigenvalues (110) into (108). The values of desired eigenvectors will be illustrated later in the paper.

In this section, multistage output feedback EA is applied to Ball and Plate system. In the first stage, the $s_1 = 8$ eigenpairs ($s_2 < n - 1$) associated with λ_x, λ_y, λ_ϕ and λ_θ are assigned using the right allowable subspace. In the second stage, the remaining $s_2 = 2$ eigenparis ($s_2 \leq r$) associated with λ_h are assigned using the left allowable subspace. As argued in Section 4, the eigenvectors assigned from the left allowable subspace should be improved compared with those assigned via full state feedback EA and conventional output-lifting EA.

To show the efficacy of the scheme, the desired left and right eigenvectors and those achieved using single rate full state feedback EA (G. P. Liu & Patton, 1998; White, 1995), output-lifting EA (L. Chen et al., 2017) and multistage output-lifting EA are presented in this section. The comparison results are shown in Table. 2. where it can be seen (in particular the bold part) that the left eigenvectors, assigned using state feedback EA and conventional output-lifting EA, can be further improved via multistage output-lifting EA and the desired left eigenvectors can be exactly assigned. In addition, the right eigenvectors, assigned (in the first stage) via full state feedback EA, output-lifting EA and proposed multistage output-lifting EA, are the same due to the invariance of the dimension of the right allowable subspace.

Table 2. A comparison of achieved eigenvectors

	Right eigenvectors (V_1)				Left eigenvectors (W_2)
Desired	$0.7071 \pm 0.0000i$	$0.0000 + 0.0000i$	$0.0000 + 0.0000i$	$0.0015 \pm 0.0369i$	$0.0000 + 0.0000i$
	$-0.5657 \mp 0.4243i$	$0.0000 + 0.0000i$	$0.0000 + 0.0000i$	$-0.0042 \mp 0.0048i$	$0.0000 + 0.0000i$
	$0.0000 + 0.0000i$	$-0.4800 \pm 0.3600i$	$0.0028 \pm 0.0278i$	$0.0000 + 0.0000i$	$0.0000 + 0.0000i$
	$0.0000 + 0.0000i$	$0.8000 + 0.0000i$	$-0.0031 \mp 0.0031i$	$0.0000 + 0.0000i$	$0.0000 + 0.0000i$
	$0.0000 + 0.0000i$	$0.0000 + 0.0000i$	$0.9876 + 0.0000i$	$0.0000 + 0.0000i$	$0.0000 + 0.0000i$
	$0.0000 + 0.0000i$	$0.0000 + 0.0000i$	$-0.1204 \pm 0.0964i$	$0.0000 + 0.0000i$	$0.0000 + 0.0000i$
	$0.0000 + 0.0000i$	$0.0000 + 0.0000i$	$0.0000 + 0.0000i$	$0.9846 + 0.0000i$	$0.0000 + 0.0000i$
	$0.0000 + 0.0000i$	$0.0000 + 0.0000i$	$0.0000 + 0.0000i$	$-0.1334 \pm 0.1067i$	$0.0000 + 0.0000i$
	$0.0000 + 0.0000i$	$0.0000 + 0.0000i$	$0.0000 + 0.0000i$	$0.0000 + 0.0000i$	$\mathbf{0.0406 \mp 0.0325i}$
	$0.0000 + 0.0000i$	$0.0000 + 0.0000i$	$0.0000 + 0.0000i$	$0.0000 + 0.0000i$	$\mathbf{0.9986 + 0.0000i}$
State feedback EA	$-0.0134 \pm 0.0216i$	$-0.0002 \pm 0.0002i$	$-0.5600 \mp 0.4200i$	$0.0000 \mp 0.0000i$	$0.0000 \mp 0.0000i$
	$-0.0191 \mp 0.1613i$	$-0.0001 \mp 0.0015i$	$0.7000 + 0.0000i$	$0.0000 \pm 0.0000i$	$0.0000 \mp 0.0000i$
	$-0.0001 \pm 0.0001i$	$0.0177 \mp 0.0297i$	$-0.0000 \pm 0.0000i$	$-0.7974 + 0.0000i$	$0.0000 \mp 0.0000i$
	$-0.0001 \mp 0.0008i$	$0.0273 \pm 0.1973i$	$-0.0000 \mp 0.0000i$	$0.4785 \mp 0.3588i$	$0.0000 \mp 0.0000i$
	$0.1180 \pm 0.0946i$	$0.0009 \pm 0.0009i$	$-0.0799 \pm 0.0602i$	$-0.0000 \mp 0.0000i$	$-0.0000 \mp 0.0000i$
	$-0.9747 + 0.0000i$	$-0.0075 \mp 0.0007i$	$0.0277 \mp 0.0963i$	$-0.0000 \pm 0.0000i$	$-0.0000 \mp 0.0000i$
	$-0.0005 \mp 0.0005i$	$0.1299 \pm 0.1042i$	$-0.0000 \mp 0.0000i$	$0.0179 \mp 0.0616i$	$-0.0000 \pm 0.0000i$
	$0.0046 \pm 0.0001i$	$-0.9651 + 0.0000i$	$-0.0000 \mp 0.0000i$	$0.0170 \pm 0.0450i$	$-0.0000 \mp 0.0000i$
	$0.0000 \pm 0.0000i$	$0.0000 \pm 0.0000i$	$-0.0000 \pm 0.0000i$	$-0.0000 \pm 0.0000i$	$\mathbf{0.9987 + 0.0000i}$
	$-0.0000 \pm 0.0000i$	$-0.0000 \mp 0.0000i$	$0.0000 \mp 0.0000i$	$-0.0000 \mp 0.0000i$	$\mathbf{0.0411 \pm 0.0309i}$
Output−lifting EA	$-0.0134 \pm 0.0216i$	$-0.0002 \pm 0.0002i$	$-0.5600 \mp 0.4200i$	$0.0000 \mp 0.0000i$	$0.0000 \mp 0.0000i$
	$-0.0191 \mp 0.1613i$	$-0.0001 \mp 0.0015i$	$0.7000 + 0.0000i$	$0.0000 \pm 0.0000i$	$0.0000 \mp 0.0000i$
	$-0.0001 \pm 0.0001i$	$0.0177 \mp 0.0297i$	$-0.0000 \pm 0.0000i$	$-0.7974 + 0.0000i$	$0.0000 \mp 0.0000i$
	$-0.0001 \mp 0.0008i$	$0.0273 \pm 0.1973i$	$-0.0000 \mp 0.0000i$	$0.4785 \mp 0.3588i$	$0.0000 \mp 0.0000i$
	$0.1180 + 0.0946i$	$0.0009 \pm 0.0009i$	$-0.0799 \pm 0.0602i$	$-0.0000 \mp 0.0000i$	$-0.0000 \mp 0.0000i$
	$-0.9747 + 0.0000i$	$-0.0075 \mp 0.0007i$	$0.0277 \mp 0.0963i$	$-0.0000 \pm 0.0000i$	$-0.0000 \mp 0.0000i$
	$-0.0005 \mp 0.0005i$	$0.1299 \pm 0.1042i$	$-0.0000 \mp 0.0000i$	$0.0179 \mp 0.0616i$	$-0.0000 \pm 0.0000i$
	$0.0046 \pm 0.0001i$	$-0.9651 + 0.0000i$	$-0.0000 \mp 0.0000i$	$0.0170 \pm 0.0450i$	$-0.0000 \mp 0.0000i$
	$0.0000 \pm 0.0000i$	$0.0000 \pm 0.0000i$	$-0.0000 \pm 0.0000i$	$-0.0000 \pm 0.0000i$	$\mathbf{0.9987 + 0.0000i}$
	$-0.0000 \pm 0.0000i$	$-0.0000 \mp 0.0000i$	$0.0000 \mp 0.0000i$	$-0.0000 \mp 0.0000i$	$\mathbf{0.0411 \pm 0.0309i}$
Multistage output −lifting EA	$-0.0134 \pm 0.0216i$	$0.0002 \mp 0.0002i$	$-0.5599 \mp 0.4198i$	$-0.0000 \mp 0.0002i$	$-0.0000 \mp 0.0000i$
	$-0.0191 \mp 0.1613i$	$-0.0000 \pm 0.0018i$	$0.7001 + 0.0000i$	$0.0001 \pm 0.0001i$	$-0.0000 \mp 0.0000i$
	$-0.0001 \pm 0.0001i$	$-0.0177 \pm 0.0297i$	$-0.0006 \mp 0.0008i$	$0.7974 + 0.0000i$	$-0.0000 \mp 0.0000i$
	$0.0001 \mp 0.0008i$	$-0.0273 \mp 0.1973i$	$0.0010 \pm 0.0003i$	$-0.4785 \pm 0.3588i$	$-0.0000 \mp 0.0000i$
	$0.1180 \pm 0.0946i$	$-0.0009 \mp 0.0010i$	$-0.0800 \pm 0.0603i$	$-0.0000 \mp 0.0000i$	$-0.0000 \pm 0.0000i$
	$-0.9747 + 0.0000i$	$0.0075 \pm 0.0007i$	$0.0278 \mp 0.0964i$	$0.0000 \mp 0.0000i$	$-0.0000 \mp 0.0000i$
	$-0.0005 \mp 0.0005i$	$-0.1299 \mp 0.1041i$	$0.0001 \mp 0.0001i$	$-0.0179 \pm 0.0616i$	$0.0000 \pm 0.0000i$
	$0.0046 \pm 0.0001i$	$0.9651 + 0.0000i$	$-0.0001 \pm 0.0001i$	$-0.0170 \mp 0.0450i$	$-0.0000 \pm 0.0000i$
	$0.0000 \pm 0.0000i$	$-0.0000 \mp 0.0000i$	$-0.0000 \pm 0.0000i$	$-0.0000 \mp 0.0000i$	$\mathbf{0.0406 \mp 0.0325i}$
	$-0.0000 \pm 0.0000i$	$0.0000 \pm 0.0000i$	$0.0000 \mp 0.0000i$	$0.0000 \mp 0.0000i$	$\mathbf{0.9986 + 0.0000i}$

Table 3. A comparison of achieved eigenvalues

	Desired	State feedback EA	Output−lifting EA	Output−lifting EA	Multistage output −lifting EA
Eigenvalues	$0.9682 \pm 0.0232i$	$0.9682 \pm 0.0232i$	$0.9682 \pm 0.0232i$	$0.9682 \pm 0.0232i$	$0.9682 \pm 0.0232i$
	$0.9761 \pm 0.0176i$	$0.9761 \pm 0.0176i$	$0.9761 \pm 0.0176i$	$0.9761 \pm 0.0176i$	$0.9761 \pm 0.0176i$
	$0.8083 \pm 0.1304i$	$0.8083 \pm 0.1304i$	$0.8083 \pm 0.1304i$	$0.8083 \pm 0.1304i$	$0.8083 \pm 0.1304i$
	$0.8266 \pm 0.1199i$	$0.8266 \pm 0.1199i$	$0.8266 \pm 0.1199i$	$0.8266 \pm 0.1199i$	$0.8266 \pm 0.1199i$
	$0.4868 \pm 0.2534i$	$0.4868 \pm 0.2534i$	$0.4868 \pm 0.2534i$	$0.4868 \pm 0.2534i$	$0.4868 \pm 0.2534i$

It is also clear from Table. 3, multistage output-lifting EA has the capability to assign the desired eigenvalues as those assigned via full state feedback EA.

The closed-loop system responses are shown in Figures 5 to 8. Figure 5 shows the position and the velocity responses of the ball along the x- and y-axes, to a unit step reference command along the x-axis. The plots exhibit the desired second-order characteristics, which are compatible with the predefined system modes, and the settling time of the x-position is close to $5sec$ (4/0.8). Figure 6 shows the angular position and velocity responses of the plant along the x- and y-axis following a unit step reference command along the x-axis. It also shows the height of the ball following a unit step reference command along the x-axis. It is clear that the height of the ball is maintained at a constant, zero-error value. Figure 7 shows the position and the velocity responses of the ball along the x- and y-axes, to a unit step reference command along the y-axis. The second-order response of the y-position is shown to be as required. The settling time is close to $6.6sec(4/0.6)$. Figure 8 depicts the angle and angular velocity responses of the plant along the x-axis and the y-axis following a unit step reference command along the y-axis. The height of the ball is maintained at a fixed height to a unit step command along the y-axis. It is clear from Figures 5 to 8 that

appropriate system modes are well decoupled. Furthermore, the system outputs are able to track given reference commands.

7. Conclusions

In this paper, a multistage output-lifting EA scheme is developed. Compared with conventional output-lifting EA, the left allowable subspace is exploited in this scheme, which allows eigenvector assignment to be further improved. In addition, the mathematical model of a novel Ball and Plate system is developed. Based upon the physical characteristics of the system, an ideal eigenstructure is derived, which allows natural modes to be distributed and decoupled in appropriate states or outputs. Since Ball and Plate is a typical multirate output feedback system with restricted DoF, it is an ideal candidate to apply a multistage output-lifting EA scheme. The design and simulation results show the efficacy of the scheme.

Appendix. A
The Linearized three-motor Ball and Plate system

In the coordination system associated with (64) and (65), the continuous-time state space matrices of the three motor Ball and Plate system are

$$A_c = \begin{bmatrix} 0 & 1.0000 & 0 & 0 & 0 & 0 & 0 & 0 & 0 & 0 \\ 0 & 0 & 0 & 0 & 7.0000 & 0.2001 & 0 & 0 & 0 & 0 \\ 0 & 0 & 0 & 1 & 0 & 0 & 0 & 0 & 0 & 0 \\ 0 & 0 & 0 & 0 & 0 & 0 & -7 & -0.2001 & 0 & 0 \\ 0 & 0 & 0 & 0 & 0 & 1 & 0 & 0 & 0 & 0 \\ 0 & 0 & 0 & 0 & 0 & -11.4360 & 0 & 0 & 0 & 0 \\ 0 & 0 & 0 & 0 & 0 & 0 & 0 & 1 & 0 & 0 \\ 0 & 0 & 0 & 0 & 0 & 0 & 0 & -11.4360 & 0 & 0 \\ 0 & 0 & 0 & 0 & 0 & 0 & 0 & 0 & 0 & 1 \\ 0 & 0 & 0 & 0 & 0 & 0 & 0 & 0 & 0 & -11.4360 \end{bmatrix} \tag{113}$$

$$B_c = \begin{bmatrix} 0 & 0 & 0 \\ 0.0023 & 0.0023 & -0.0047 \\ 0 & 0 & 0 \\ -0.0070 & 0.0070 & 0 \\ 0 & 0 & 0 \\ -0.1330 & -0.1330 & 0.2660 \\ 0 & 0 & 0 \\ -0.3989 & 0.3989 & 0 \\ 0 & 0 & 0 \\ 0.0199 & 0.0199 & 0.0399 \end{bmatrix} \tag{114}$$

References

Alireza, E. A., & Batool, L. (2012). Application of matrix perturbation theory in robust control of large-scale systems. *Automatica*, *48*, 1868–1873.

Andry, A. N., Shapiro, E. Y., & Chung, J. C. (1983). Eigenstructure assignment for linear systems. *IEEE Trans. Aerosp. Electron. Syst.*, *19*, 711-727.

Awtar, S., Bernard, C., Boklund, N., Master, A., Ueda, D., & Craig, K. (2002). Mechatronic design of a ball-on-plate balancing system. *Mechatronics*, *12*, 217 - 228.

Castro, R., Flores, J. V., Salton, A. T., & Pereira, L. F. A. (2014, August). A comparative analysis of repetitive and resonant controllers to a servo-vision ball and plate system. In *Proc. 19th IFAC World Congress.* Cape Town, South Africa.

Chen, B., & Nagarajaiah, S. (2007). Linear-matrix-inequality-based robust fault detection and isolation using the eigenstructure assignment method. *AIAA Journal of Guidance, Control and Dynamics*, *30*, 1831-1835.

Chen, L., Pomfret, A., & Clarke, T. (2017). Increasing eigenstructure assignment design degree of freedom using lifting. *Int. J. Control*, *90*, 2111-2123.

Chen, T., & Francis, B. A. (1995). *Optimal sampled-data control systems*. Springer, London.

Clarke, T., Ensor, J. E., & Griffin, S. J. (2003). Desirable eigenstructure for good short-term helicopter handing qualities: the attitude command response case. *Proceedings of the Institution of Mechanical Engineers, Part G: Journal of Aerospace Engineering*, *217*, 43-45.

Clarke, T., & Griffin, S. J. (2004). An addendum to output feedback eigenstructure assignment:retro-assignment. *Int. J. Control*, *77*, 78-85.

Clarke, T., Griffin, S. J., & Ensor, J. E. (2003). Output feedback eigenstructure assignment using a new reduced orthogonality condition. *Int. J. Control*, *77*, 390-402.

Date, H., Sampei, M., Ishikawa, M., & Koga, M. (2004). Simultaneous control of position and orientation for ball-plate manipulation problem based on time-state control form. *IEEE T. Robotic. Autom.*, *20*, 465-480.

Duval, C., Clerc, G., & LeGorrec, Y. (2006). Induction machine control using robust eigenstructure assignment. *Control Eng. Pract.*, *14*, 26-43.

Fahmy, M. M., & O'Reilly, J. (1988). Multistage parametric eigenstructure assignment by output-feedback control. *Int. J. Control*, *48*, 97-116.

Fan, X., Zhang, N., & Teng, S. (2004). Trajectory planning and tracking of a ball and plate system using a hierarchical fuzzy control scheme. *Fuzzy Sets Syst.*, *144*, 297-312.

Farineau, J. (1989, December). Lateral electric flight control laws of civil aircraft based on eigenstructure assignment technique. In *Proc. AIAA Guidance, Navigation and Control Conference.* Boston, MA. USA.

Garrard, W. L., Low, E., & Prouty, S. (1989). Design of attitude and rate command systems for helicopters using eigenstructure assignment. *AIAA Journal of Guidance, Control and Dynamics*, *12*, 783-791.

Kimura, H. (1975). Pole assignment by gain output feedback. *IEEE Trans. Autom. Control*, *20*, 509-516.

Kimura, H. (1977). A further result on the problem of pole assignment by output feedback. *IEEE Trans. Autom. Control*, *25*, 458-463.

Kshatriya, N., Annakkage, U. D., Hughes, F. M., & Gole, A. M. (2007). Optimized partial eigenstructure assignment-based design of a combined PSS and active damping controller for a DFIG. *IEEE Trans. Power Syst.*, *25*, 866–876.

Lhachemi, H., Saussie, D., & Zhu, G. (2017). Explicit hidden coupling terms handling in gain-scheduling control design via eigenstructure assignment. *Control Eng. Pract.*, *58*, 1-11.

Liu, G. P., & Patton, R. J. (1998). *Eigenstructure assignment for control system design*. Wiley, Chichester.

Liu, Y., Tan, D. L., Wang, B., & Wang, X. (2013). Linear-matrix-inequality-based fault diagnosis for gas turbofan engine using eigenstructure assignment principle. *Applied Mechanics and Materials*, *302*, 759–764.

Low, E., & Garrard, W. L. (1993). Design of flight control systems to meet rotorcraft handling qualities specifications. *AIAA Journal of Guidance, Control and Dynamics*, *16*, 69-78.

Moore, B. C. (1976). On the flexibility offered by state feedback in multivariable systems beyond closed loop eigenvalue assignment. *IEEE Trans. Autom. Control*, *21*, 689-692.

Ntogramatzidis, L., Nguyen, T., & Schmid, R. (2015). Repeated eigenstructure assignment for controlled invariant subspaces. *European Journal of Control*, *26*, 1-11.

Oriolo, G., & Vendittelli, M. (2005). A framework for the stabilization of general nonholonomic systems with an application to the plate-ball mechanism. *IEEE Trans. Rob.*, *21*, 162-175.

Ouyang, H., Richiedei, D., Trevisani, A., & Zanardo, G. (2012). Discrete mass and stiffness modifications for the inverse eigenstructure assignment in vibrating systems: Theory and experimental validation. *Int. J. Mech. Sci.*, *64*, 211–220.

Patton, R. J., Liu, G. P., & Patel, Y. (1995). Insensitivity properties of multi-rate feedback control systems. *IEEE Trans. Autom. Control*, *40*, 337-342.

Piou, J., & Sobel, K. M. (1994). Yaw pointing and lateral translation using robust sampled data eigenstructure assignment. *AIAA Journal of Guidance, Control and Dynamics*, *17*, 1133-1135.

Piou, J., & Sobel, K. M. (1995). Robust multirate eigenstructure assignment with flight control application. *AIAA Journal of Guidance, Control and Dynamics*, *18*, 539-546.

Pomfret, A. J., & Clarke, T. (2009). Desirable eigenstructure for good short-term helicopter handling qualities: the rate command response case. *Proceedings of the Institution of Mechanical Engineers, Part G: Journal of Aerospace Engineering*, *223*, 1059-1065.

Pomfret, A. J., Clarke, T., & Ensor, J. (2005, July). Eigenstructure assignment for semi-proper systems: pseudo-state feedback. In *Proc. 16th IFAC World Congress, Prague.*

Roppenecker, G., & O'Reilly, J. (1989). Parametric output feedback controller design. *Automatica*, *25*, 259-265.

Srinathkumar, S. (1978). Eigenvalue/eigenvector assignment using output feedback. *IEEE Trans. Autom. Control*, *23*, 79-81.

Wahrburg, A., & Adamy, J. (2013). Parametric design of robust fault isolation observers for linear non-square systems. *Systems & Control Letters*, *62*, 420–429.

Wang, Y., Sun, M., Wang, Z., Liu, Z., & Chen, Z. (2014). A novel disturbance-observer based friction compensation scheme for ball and plate system. *ISA Transactions*, *53*, 671 - 678.

White, B. A. (1995). Eigenstructure assignment: a survey. *Proceedings of the Institution of Mechanical Engineers, Part I: Journal of Systems and Control Engineering*, *209*, 1-11.

White, B. A., Bruyere, L., & Tsourdos, A. (2007). Missile autopilot design using quasi-LPV polynomial eigenstructure assignment. *IEEE Trans. Aerosp. Electron. Syst.*, *43*, 1470-1483.

Yuan, D., & Zhang, Z. (2010). Modelling and control scheme of the ball-plate trajectory-tracking pneumatic system with a touch screen and a rotary cylinder. *IET Control Theory & Applications*, *4*, 573-589.

Zhao, L., & Lam, J. (2016a). Dominant pole and eigenstructure assignment for positive systems with state feedback. *Int. J. Syst. Sci.*, *47*, 2901-2912.

Zhao, L., & Lam, J. (2016b). Multiobjective controller synthesis via eigenstructure assignment with state feedback. *Int. J. Syst. Sci.*, *47*, 3219-3231.

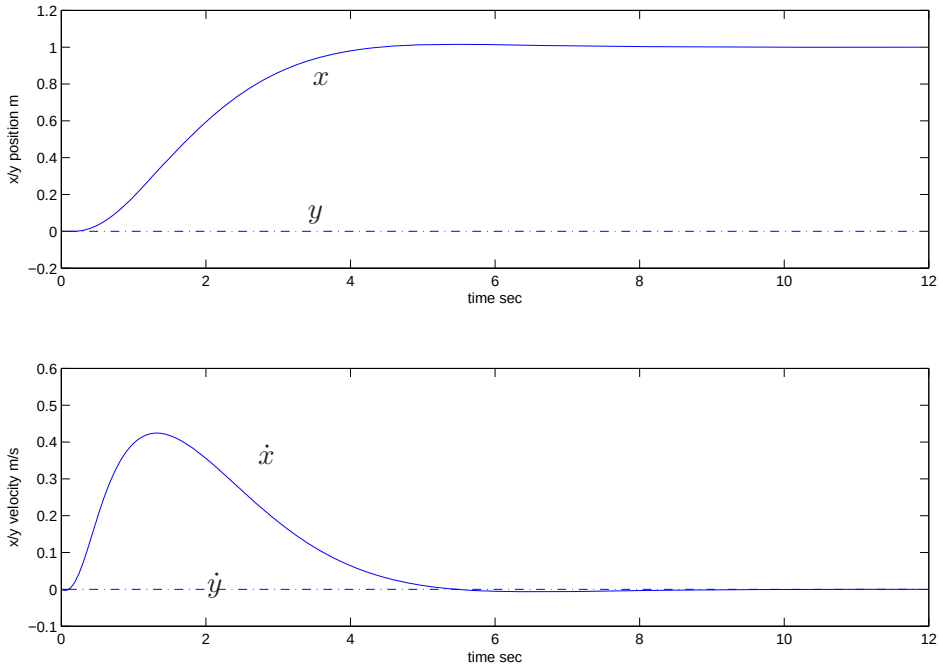

Figure 5. Response of the Closed-Loop System to a unit x-axis Position Command

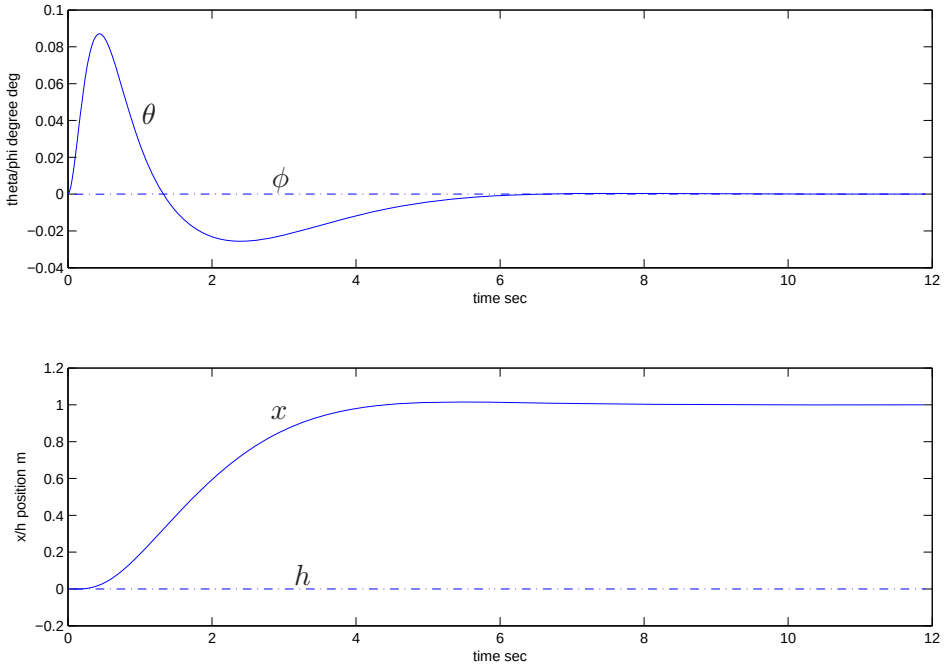

Figure 6. Response of the Closed-Loop System to a unit x-axis Position Command

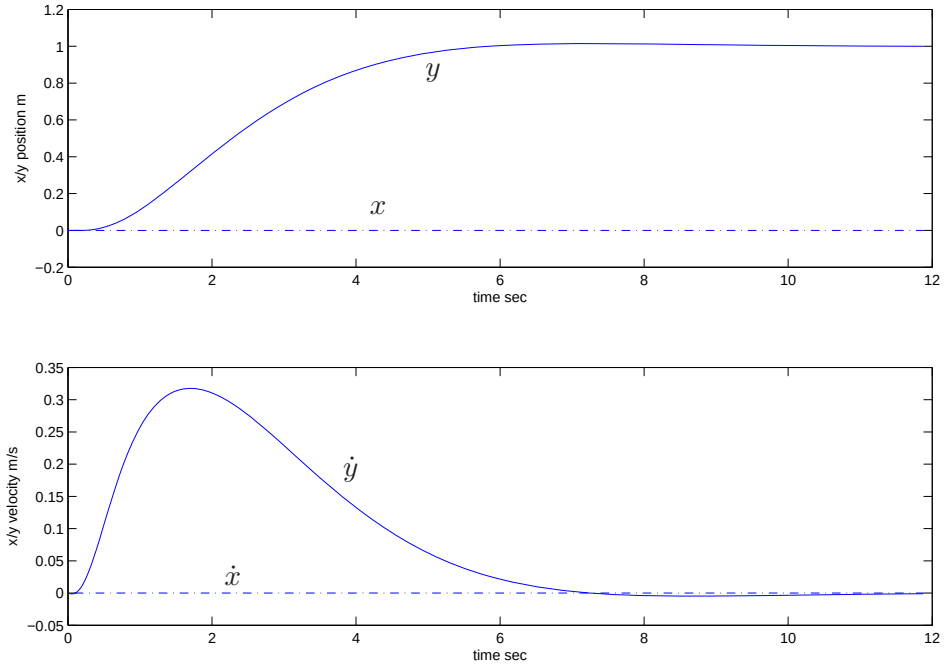

Figure 7. Response of the Closed-Loop System to a unit y-axis Position Command

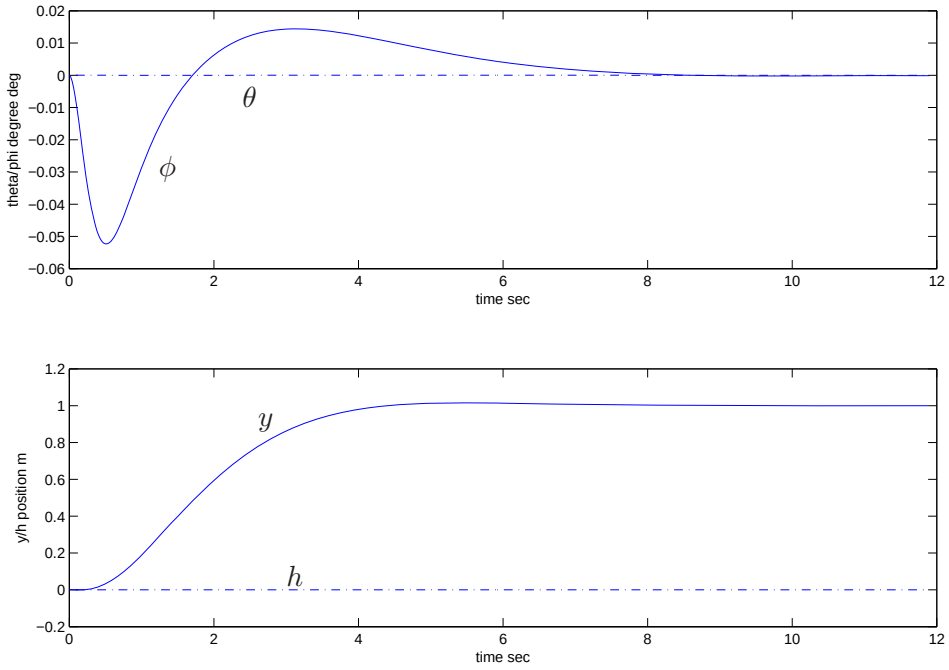

Figure 8. Response of the Closed-Loop System to a unit y-axis Position Command